Master's thesis

NTNU
Norwegian University of Science and Technology
Faculty of Engineering
Department of Energy and Process Engineering

Martin Systad Geiran

Experiments with a latent heat storage for frying

Master's thesis in Mechanical Engineering
Supervisor: Ole Jørgen Nydal
Co-supervisor: Abraham Alejandro Parra Suarez
June 2021

NTNU
Norwegian University of
Science and Technology

Martin Systad Geiran

Experiments with a latent heat storage for frying

Master's thesis in Mechanical Engineering
Supervisor: Ole Jørgen Nydal
Co-supervisor: Abraham Alejandro Parra Suarez
June 2021

Norwegian University of Science and Technology
Faculty of Engineering
Department of Energy and Process Engineering

NTNU
Norwegian University of
Science and Technology

Acknowledgments

I want to express my gratitude towards my supervisor Ole Jørgen Nydal for including me on this exciting project, providing suggestions for work and being an inspiration throughout this past year.

I also want to thank my co-supervisor Abraham Alejandro Parra Suarez, for aiding me in the lab during testing, feedback on work, discussions, as well as providing usefull information throughout the entirety of this project.

Lastly, I want to thank Paul Svendsen, Per Bjørnås Pernille Kristoffersen, Stein Kristian Stånøy, Sondre Nubdal and Martin Bustadmo, for their help with laboratory work.

This project would not have been possible without a the help of all of you.

Abstract

The object of this project, has been to test a heat storage system combined with a cooking plate, to be used for food preparation. The system is intended to be heated with excess energy or renewable energy sources in off grid locations.

The energy in the system is stored in thermal oil, and phase change materials to provide a high near constant temperature output from the system. Heat from the storage is transported to the fryer through a thermosyphon. The system does not have any moving parts, only relying on convective and gravity forces to transport heat.

The system has been heated using power grid, and solar cells to get an indication of the heating time and storing capabilities of the system. Previous numerical simulations from project work carried out in the fall of 2020, are used to compare results from experimental data.

Tests carried out in the spring of 2021 indicates that the system works as intended, and shows potential to be used as a heat storage in off grid locations. Further testing should focus on better insulation, testing over longer periods of time, like the system is intended for. Modified parts should also be tested to see how well they affect the system.

Sammendrag

Formålet med dette prosjektet har vært å teste et varmelagringssystem kombinert med en stekeplate, som skal brukes til matlaging. Systemet skal varmes med overflødig energi, eller fornybare energikilder på steder uten tilgang til et strømnett.

Energien i systemet lagres i termisk olje, og faseendringsmaterialer slik at systemet kan ha en høy nær konstant temperatur under bruk. Varme fra lageret transporteres til stekeplaten gjennom en termosyfon. Det er ingen bevegelige deler i systemet, of varmefordelingen skjer gjennom konveksjons- og tyngdekrefter.

Systemet har gjennom tester blitt varmet opp med strøm fra strømnettet og solcellepaneler. Resultater fra disse testene vil gi en indikasjon på oppvarmingstid, og lagringskapasiteten til systemet. Numeriske simuleringer fra prosjekarbeid utført høsten 2020, brukes til å sammenligne resultater fra eksperimentelle data.

Tester gjennomført våren 2021 indikerer at systemet fungerer som ønsket, og viser potensiale for å bli brukt til vamrelagring i steder uten tilgang til et strømnett. Videre testing burde fokusere på å bedre isolasjon av systemet, å teste over lengre perioder slik som systemet er tiltenkt å brukes. Modifiserte deler, burde også bli testet for å se effekten av disse.

Content

List of Figures

List of Tables

Nomenclature

Abbreviations

HTF	Heat transfer fluid
LHS	Latent Heat Storage
PCM	Phase Change Material
PV	Photo Voltaic
SHS	Sensible Heat Storage
TPCT	Two-Phased Closed Thermosyphon

Symbols

Δh	Enthalpy change	j/kg
ΔT	Temperature change	$°C$
μ	Dynamic viscosity	cP
ρ	Density	kg/m^3
c_p	Specific heat capacity	$j/kg\,K$
k	Thermal conductivity	$W/m\,K$
m	Mass	kg
Q	Heat	j
T	Temperature	$°C$
V	Volume	m^3
I	Electric current	A
n	Number of instances	-
P	Power	W
R	Electric resistance	Ω
U	Voltage	V

1 Introduction

1.1 Background

Having access to electricity is something a lot of people take for granted. Not everyone however, has access to electricity. Numbers from 2019, showed that nearly 600 million people living in sub-Saharan Africa did not have access to electricity, after having a steady decline during the last decade. However the number of people without access to electricity *increased* in 2020, due to the Covid-19 pandemic.[1]

Du to the lack of electric energy, many households in sub-Saharan Africa relies heavily on fossil fuels for food preparation. Burning fuels indoors has disadvantages, such as bad indoor climate which is linked to respiratory illnesses[7][13]. The use of firewood for heating, is also a cause of deforestation, which can have a negative impact on the local ecosystem. This has created an incentive to provide healthy as well as environmentally friendly food preparation options in areas without access to an electric grid.

The use of renewable energy, is limited by the access of it. Sometimes when the energy is needed, it is not there. Other times, where it is a lot of it the available storing capacity does not allow for everything to be captured. Hence there is a need to store this energy when it is available. Heat storages can be an effective way of storing energy, in times where battery capacity is not sufficient. This project aims to make a heat storage combined with a cooking application, that stores renewable energy in times of abundance.

1.2 Project description

The following tasks are to be carried out in this work:

- Demonstrate heating functionality of latent heat storage using power grid
- Demonstrate discharging functionality of latent heat storage
- Demonstrate functionality of latent heat storage using PV-panels
- Realize eventual modifications to latent heat storage to improve quality of system
- Compare experimental to numerical results of system

1.3 Objective

The objective for this project is to establish an effective system that can use solar energy to store heat, and later release this heat at a sufficiently high near-constant temperature,

for it to be used for food preparation. A prototype system has been built for experimental purposes, and will be tested this spring. The system will be tested under conditions close to the intended operating conditions, and monitored to see the effectiveness of the system.

Should the tests uncover flaws of the prototype system, modifications will be discussed and built to better the overall effectiveness and robustness of the system.

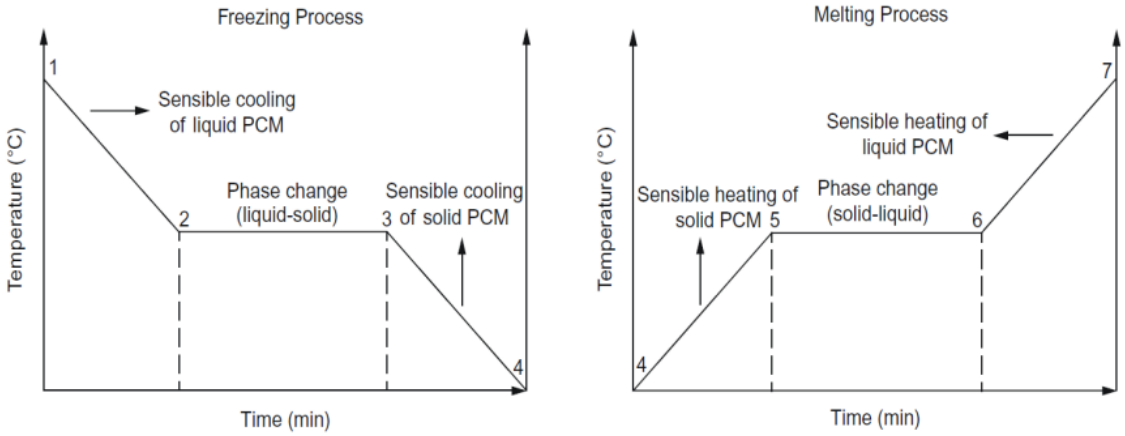

Figure 1: Heat storing and release process of PCM [12]

2 Theory

2.1 Thermal energy storage

A thermal energy storage (TES) is a way of storing energy, in the form of heat. Energy can be stored as both sensible heat (SHS) and latent heat (LHS). An SHS utilizes the heat capacity of a substance, and the heat is stored through a temperature change. A latent heat storage on the other hand, utilizes the difference in enthalpy of the solid and liquid phase of a substance in addition to sensible heat, giving an LHS a much higher storage density[18].

The substances used in an LHS is commonly refered to as phase change materials (PCM)[14]. Since heat exchange associated with latent heat transfer, the process does not inflict a temperature change like for sensible heat [21]. For a substance to be used as a PCM in an LHS it needs to have a suitable melting temperature as well as a large phase change enthalpy. The sensible and latent heat exchange is illustrated in Figure 1.

2.1.1 Capturing and releasing Solar Energy

There are multiple ways of capturing solar energy, such as the use of photo voltaic panels (PV panels), which will be a topic in this report. The system in this report, is intended to use solar power from PV panels, to give power to a heating element. This heating element, will in turn charge a heat storage, so that this heat can be used for food preparation.

To make use of the thermal energy stored in a heat storage, there needs to be a way to extract it. The temperature output of a thermal energy storage depends on the area of

Thermophysical property	Value
Density (kg/m3)	
Temperature $< 220°C$	1800
Temperature $\geq 220°C$	1700
Enthalpy of fusion (kj/kg)	108.67
Phase transition enthalpy (kj/kg)	31.9

Table 1: Thermophysical properties of solar salt mixture

use. Due to food preparation requiring a high temperature output, the heat storage in this report needs to store thermal energy at a high temperature.

2.2 Phase Change Materials

Phase Change Materials (PCM), refer to materials that can absorb and release large amounts of latent heat at a near constant temperature when experiencing a phase change, i.e. going from a liquid to a solid or vice versa. Depending on the material, PCM can therefore be used to store energy in a chosen temperature range[8]. For PCM, the latent heat is a lot higher than the sensible heat for the same substance. In this project, the PCM is a binary homogeneous mixture of $NaNO_3 - KNO_3$, with a molar ratio of 60:40 respectively. The modified heat capacity of the current mixture of salts is showed in Equation 2, which in turn is depicted in Figure 2[9].

Comparing the thermodphysical properties of the PCM used in this report in Table 1 to its heat capacity, one can see that the enthalpy of fusion is far higher than the heat capacity. This means that heating the substance 1°C, stores about ten times less heat than the latent heat stored in the phase change.

The overall storing capacity of a PCM, can be expressed as in Eq. 1 [19]:

$$Q_{PCM} = \int_{T_i}^{T_m} mc_p dT + m\Delta h_m + \int_{T_m}^{T_f} mc_p dT \tag{1}$$

m is the mass of the substance.
c_p is the heat capacity of the substance at a constant pressure.
T_i, T_m and T_f are the initial, melting and final temperature respectively.
Δh_m is the enthalpy change of the substance per unit mass

The thermophysical properties of the PCM used in this project can be seen in Table 1[9].

$$c_p[kj/kgK] = \begin{cases} 0.75 & \text{if } T < 110°C \\ 4.1 & \text{if } 110 \leq T \leq 120°C \\ 1.4 & \text{if } 120 \leq T \leq 210°C \\ 12 & \text{if } 210 \leq T \leq 220°C \\ 1.6 & \text{if } T > 220°C \end{cases} \tag{2}$$

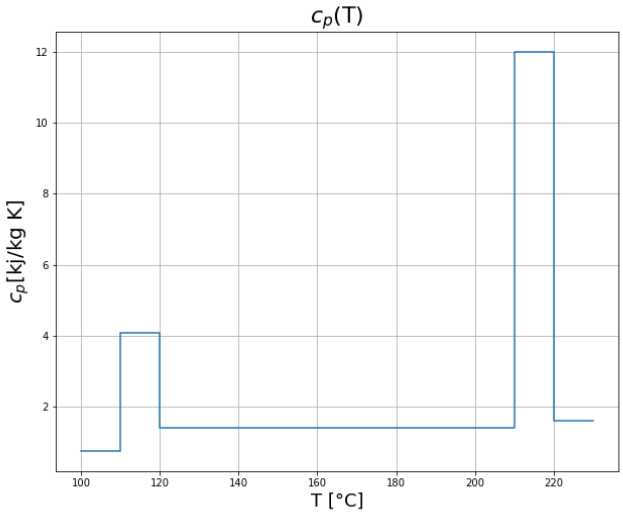

Figure 2: Approximate heat capacity for solar salt used in this project [16]

2.3 Heat Transfer Fluid

The heat transfer in the system, is carried by a heat transfer fluid (HTF). In addition to transferring heat between different components in the system, a heat transfer fluid can store sensible heat, increasing the storing capacity of the system.

The working fluid used in the current system is Duratherm 630. This is a fitting working fluid, as the maximum temperature of the oil is 332°C / 630°F , which is well within the maximum temperature of this system. It is also non toxic, making it suited for indoor use. Sunflower oil was also considered as HTF for this system, however it was decided against with regard to the longevity of the system. The deciding factor to choosing Duratherm, is that sunflower oil has a great increase in viscosity when exposed to air[20]. This increase in viscosity makes it so that the oil needs to be replaced, and the system needs to be cleaned regularly. To reduce the requirement for maintenance, Duratherm 630 has been used, as it does not have the same characteristic.

Due to a low thermal conductivity (ref Tab. 2), the main source of heat transfer in the system comes from fluid movement created in the oil induced by temperature differences, which is true for most liquids[15].

The relevant quantities of the fluid from Table 2, are taken from Appendix A [3]

T [° C]	ρ $[kg/m^3]$	k $[W/m\,K]$	c_p $[kJ/kg\,K]$	μ $[cP]$
25	862.23	0.144	1.948	75.34
55	841.84	0.142	2.047	19.76
105	807.84	0.140	2.212	4.97
155	773.84	0.137	2.377	2.13
185	753.45	0.135	2.476	1.47
225	726.25	0.133	2.608	0.99

Table 2: Relevant quantities for Duratherm 630

2.4 Available energy of the storage

To calculate the theoretical storing capacity of the system, one has to calculate the energy storing capacity in the oil, and PCM for the system.

The energy in the oil, can be calculated through Eq. 3.

$$Q_{theoretical} = m \cdot c_{p,oil} \cdot \Delta T \tag{3}$$

Where, in Eq. 3:

$$m = \rho V \tag{4}$$

Combining Eqs. 1 and 3:

$$Q_{total} = Q_{PCM} + Q_{oil} \tag{5}$$

The mass of the PCM in the cylinders, is calculated to be $1.944kg$ per cylinder, and the volume of the oil in the tank is calculated to be $75l$, without the PCM rods. This value is used so that with the expansion of oil during heating, the tank will be close to filled with this amount. Using these quantities, and having $T_1 = 25°C$, the total energy storing capacity of the system is presented in Table 3.

Where the mass of the PCM for the two cases in Tables 3, 4 and 5 is given as:

$$m_{PCM} = 11.66kg, \text{ for } n_{PCM} = 6$$
$$m_{PCM} = 31.10kg, \text{ for } n_{PCM} = 16$$

And the initial volume of Duratherm is given as follows:

$$V_{oil} = 0.075 - (n_{PCM} * 1.08 * 10^{-3}) \quad [m^3]$$

This volume is determined by the initial values of the system, meaning that the total mass of oil in the system can be expressed as in Equation 6:

$$m_{oil} = V_{oil} * 862.23 \quad [kg] \tag{6}$$

Where $862.23[kg/m^3]$, is the density of Duratherm 630 at 25°C, collected from Table 2.

Temperature[°C]	0 PCM cylinders		6 PCM cylinders		16 PCM cylinders	
	Capacity[kj]	diff[%]	Capacity[kj]	diff[%]	Capacity[kj]	diff[%]
25-100	9 700.09	0 %	9 914.64	2 %	10 272.23	6 %
25-160	17 460.16	0 %	17 846.35	2 %	18 490.01	6 %
25-200	22 633.54	0 %	23 134.16	2 %	23 968.54	6 %
25-210	23 926.88	0 %	24 456.11	2 %	25 338.17	6 %
25-230	26 513.57	0 %	28 376.88	7 %	31 482.38	19 %

Table 3: Storing capacity of system, with different PCM configurations

2.4.1 Storing capacity different temperature ranges

The difference in total storing capacity between utilizing and not utilizing PCM, can be seen in Table 3. For low temperature ranges, this difference is not to big, however looking at higher temperature ranges, such as $T_i = 160°C$, $T_f = 230°C$, the storing capacity is greatly different. Table 5, shows that using 16 PCM cylinders in the system, increases the overall storing capacity of 44% in the temperature range 160°C-230°C.

Temperature[°C]	0 PCM cylinders		6 PCM cylinders		16 PCM cylinders	
	Capacity[kj]	diff [%]	Capacity[kj]	diff [%]	Capacity[kj]	diff [%]
100-200	12 933.45	0 %	13 219.52	2 %	13 696.31	6 %
100-210	14 226.80	0 %	14 541.47	2 %	15 065.94	6 %
100-230	16 813.49	0 %	18 462.24	10 %	21 210.15	26 %

Table 4: Storing capacity of system, with different PCM configurations, in range $T_i = 100°C$ to $T_f = 230°C$

The results in Tables 3, 4 and 5, is calculated using Equation 7.

$$Q = \begin{cases} m_{oil}c_{p,oil}(T_f - T_i) + m_{PCM}c_{p,PCM}(T_f - T_i) & \text{, for } T < 220°C \\ m_{oil}c_{p,oil}(T_f - T_i) + m_{PCM}c_{p,PCM}(T_f - T_i) + m_{PCM}\Delta h & \text{, for } T \geq 220°C \end{cases} \tag{7}$$

Temperature[°C]	0 PCM cylinders		6 PCM cylinders		16 PCM cylinders	
	Capacity[kj]	diff [%]	Capacity[kj]	diff [%]	Capacity[kj]	diff [%]
160-200	5 173.38	0 %	5 287.81	2 %	5 478.52	6 %
160-210	6 466.73	0 %	6 609.76	2 %	6 848.15	6 %
160-230	9 053.42	0 %	10 530.52	16 %	12 992.37	44 %

Table 5: Storing capacity of system, with different PCM configurations, in range $T_i = 160°C$ to $T_f = 230°C$

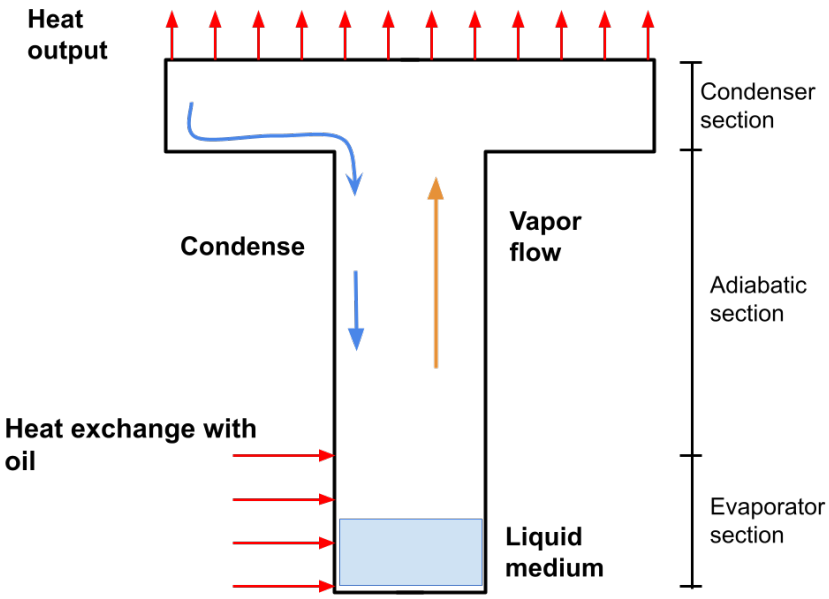

Figure 3: Drawing showing how the thermosyphon works for this setup

2.5 Thermosyphon

The system in this report, utilizes a two-phased closed thermosyphon (TPCT), which is an enclosed pipe with a liquid medium inside[11]. For experiments performed in this report, the medium is propylene glycol.

The way a TPCT works, is that liquid inside the pipe is being heated in the evaporator section. When the liquid reaches its saturation temperature, it evaporates. This vapour then rises due to gravity forces in the pipe, entering the inside of the cooking plate, which is the condenser section of this thermosyphon. In the condenser, the vapor exchanges heat with the surroundings and condenses, in this case the cooking plate. The condensate, then falls back through the pipe, into the evaporator section. This process is shown in Figure 3.

To lower the evaportaion temperature and pressure forces within the thermosyphon, the propylene glycol is stored in a vaccum. This requires the system to be fully closed, not letting in any air, as this would reduce the functionality of the heat pipe.

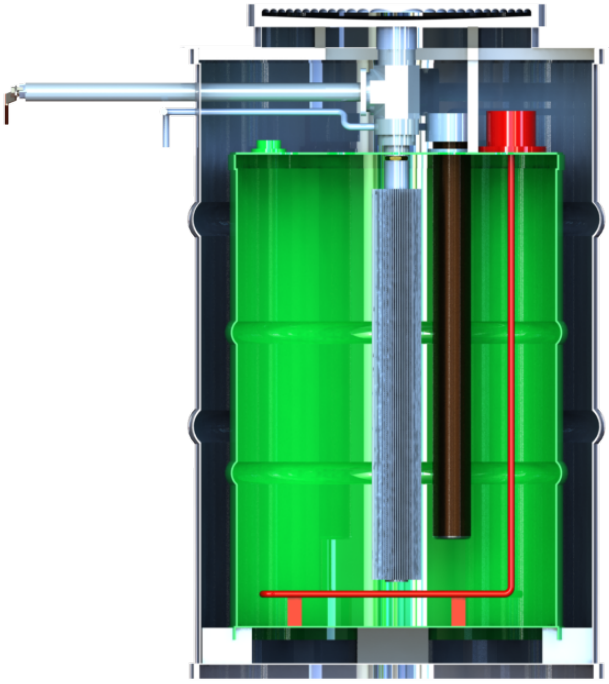

Figure 4: 3D model of the protoype system [17]

3 System

This section will describe the current system, that has been built as well as the test setup used to obtain data on the current prototype system.

3.1 Initial system

Figure 4, shows a 3D, model of the initial system that has been built and tested for this project.It contains several components, which will be listed and explained in this chapter.

1. Heating element
2. Heat transfer fluid
3. Plate
4. Heat pipe
5. Valve
6. PCM cylinders

Figure 5: Picture of the current prototype system

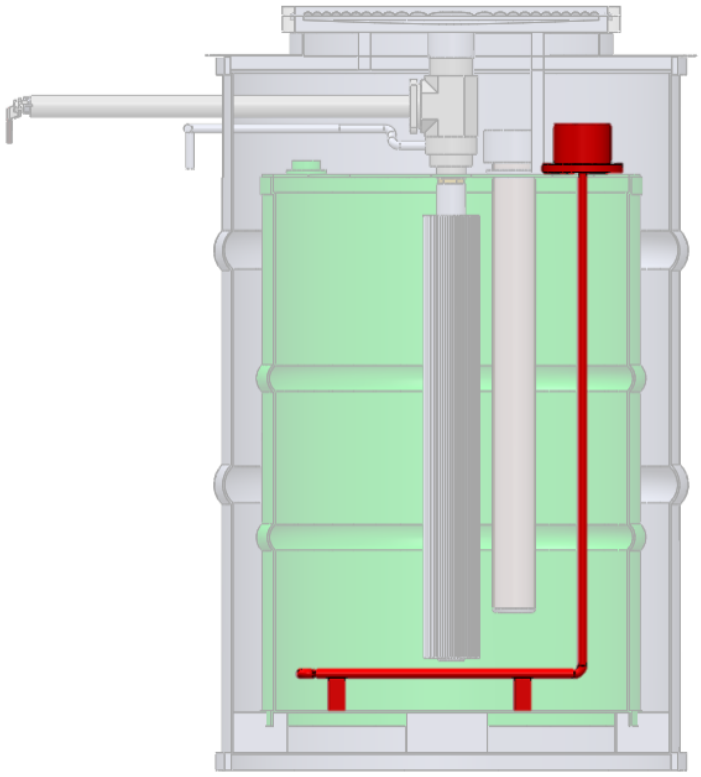

Figure 6: Heating element highlighted in system

3.1.1 Heating Element

The energy source of the system, is a heating element shown in Figure 6. The heating element is powered by electricity, which is intended to come from renewable resources, however for the majority of testing performed this spring, the element has been connected to the power grid.

Figure 7, shows a picture of the heating element identical to the one used for this project. Only the lowermost part of the heating element is active, meaning that the system is heated from the bottom. This way the heat in the storage is distributed in the system through convective forces.

A voltage of 230V on the heating element corresponds to 1800W of power. The maximum voltage used for the experiments conducted this spring, has been 220V. Assuming that the resistance of the heating element is constant, and that the power follows $P = U * I$, this voltage corresponds to a power output of 1721W[4].

Figure 7: Picture of a heating element identical to the one used in the current system

3.1.2 Heat Transfer Fluid

The innermost tank, is filled with a heat transfer fluid called Duratherm 630. This heat transfer fluid, serves two purposes; to store heat, and distribute heat in the storage to other working components. The datasheet for Duratherm 630 can be found in Appendix A.

When the system is in use, temperature differences in the oil will occur due to heating or cooling. These temperature differences gives rise to convective forces in the oil, which in turn creates fluid movement. These convective forces is what drives the heat transfer as mentioned in Section 2.3

3.1.3 Plate and Heat Pipe

To transport heat from the heat storage to the cooking plate, the system utilizes a thermosyphon principle, explained in Section 2.5. Figure 8 shows that the heat pipe as well as plate, is hollow. The inside of the pipe and plate, contains 230 mL of propylene glycol, which is the working fluid in the thermosyphon. The transport of heat from the storage to the plate, starts with the oil exchanging heat with the heat pipe. When the propylene reaches its boiling temperature, it evaporates. This vapor then rises to the underside of the plate due to gravity forces. After reaching the underside of the plate, the vapor will condense, before flowing back into the thermosyphon for the cycle to repeat.

The inside of the plate is constructed with grooves to better the thermal conductivity from the storage, as well as provide space for the vapor to condense on. These grooves are shown in Figure 9

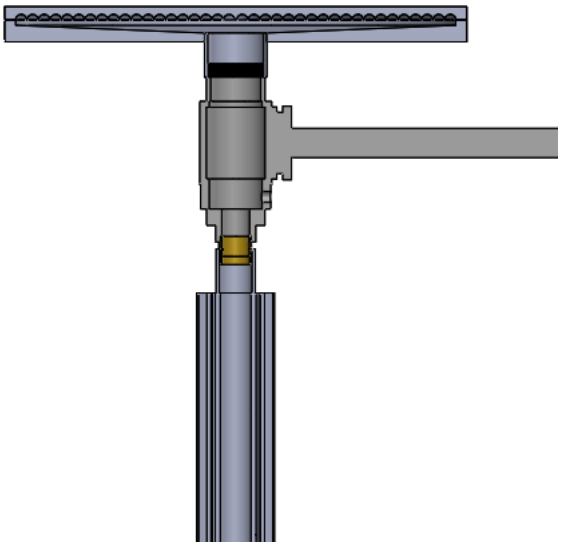

Figure 8: Thermosyphon and plate cut section view

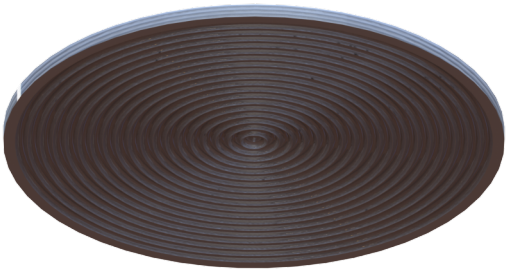

Figure 9: Showing the grooves on the underside of the top plate

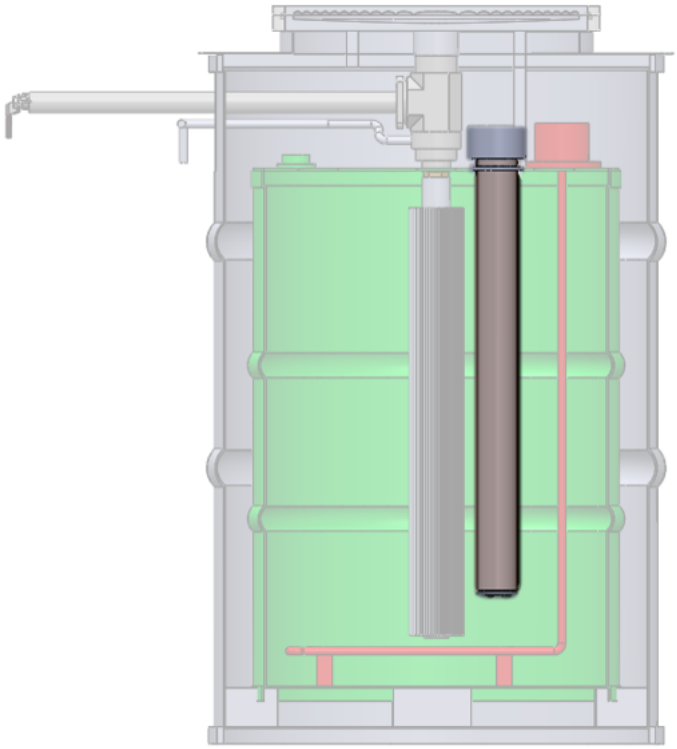

Figure 10: Location of PCM cylinders highlighted in system

3.1.4 Valve

To restrict heat flow from storage to plate, the junction between the plate and heat pipe consists of a high temperature ball valve. The idea, is that the valve can be closed so that the vapor flow from the bottom of the thermosyphon can no longer reach the underside of the plate, making it possible to reduce the plate temperature when the system is charged.

3.1.5 PCM Cylinders

The system utilizes phase change materials, which is stored in cylinders connected in the top of the inner tank. The location of these are shown in Figure 10. The amount of PCM cylinders in the system can be altered by inserting or removing cylinders, with a maximum amount of cylinders for this system, set to 16 cylinders.

During experiments performed this spring, the amount of cylinders in the system has been limited to 6.

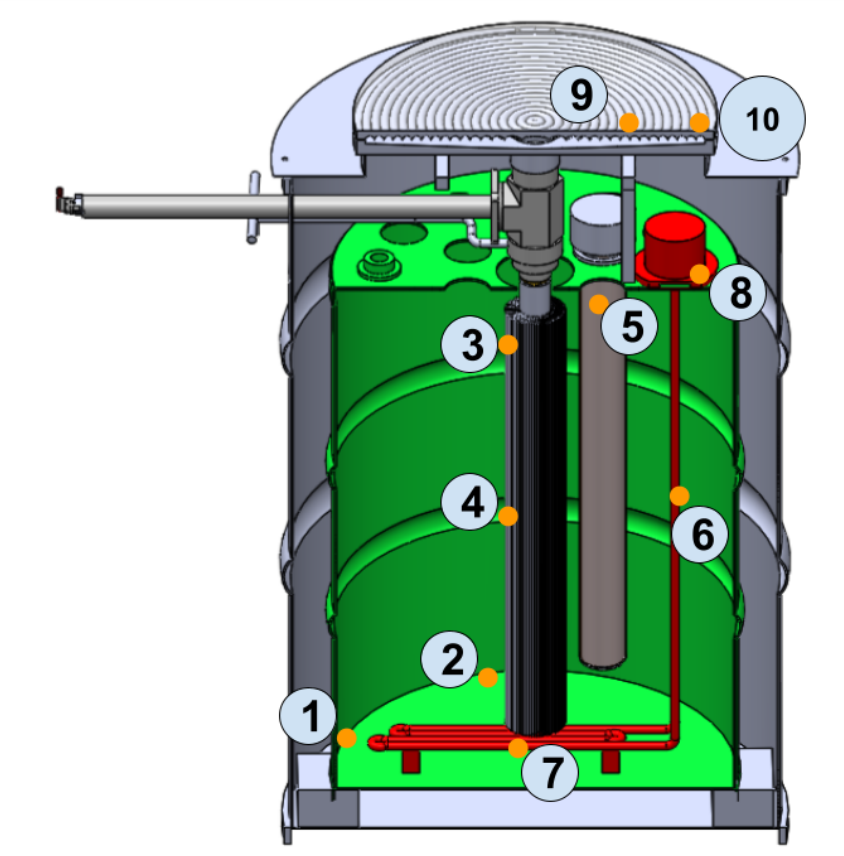

Figure 11: Numbered locations of the different thermocouples

3.2 Thermocouples

To log the temperature development in the system, thermocouples were placed at several points in the system. Figure 11, shows the location of the thermocouples while Table 6, connects the numbers to the corresponding thermocouple labels used in Section 5.

The temperatures were logged using PicoLog 6, and two different loggers, shown in Figure 12.

Number	Name
1	Oil Bottom 1
2	Oil Bottom 2
3	Fins Top
4	Fins Middle
5	Salt Top
6	HE Middle
7	HE Bottom
8	HE Metal Box
9	Plate Middle
10	Plate Radius

Table 6: Table mapping thermocouple locations to correct label name in plots

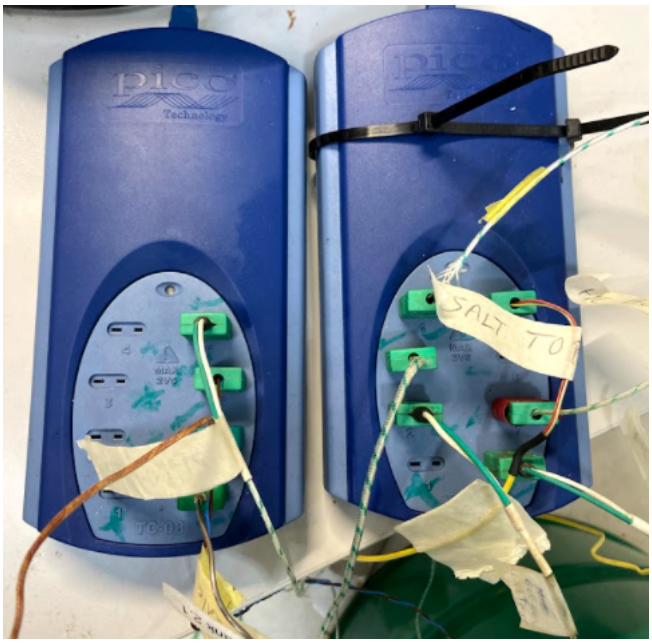

Figure 12: The loggers used for testing in this project

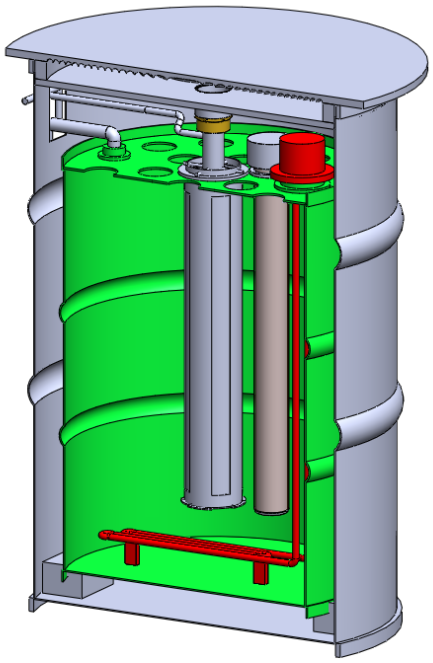

Figure 13: 3D model of the modified system

3.3 Modified system

Due to certain limitations that were encountered in the initial system, modifications has been made. The modifications made, has been made regarding safety, energy efficiency, robustness, reduced maintenance, easier build and longevity of the final system. The modifications as well as the reasoning behind the individual modifications, will be listed below.

Results from testing of the modified system, will be presented in section 6.3.

3.3.1 Modified valve

The initial valve of the system, requires several junctions between the heat pipe and plate, which makes the system prone to leakage. This, combined with the fact that the valve itself is an expensive part, resulted in the decision to try to make a replacement to the initial valve.

The idea became to make a separator pipe, to encapsulate the heat pipe. This way one could potentially restrict heat flow from the oil to the heat pipe. The separator pipe consists of two pipes, where one is put inside the other. Slits were cut along the sides of the pipe, and blade-like caps were put on the bottom. This way, the separator pipe could open and close by twisting the pipes in opposite directions. This mechanism is illustrated in Figure 14.

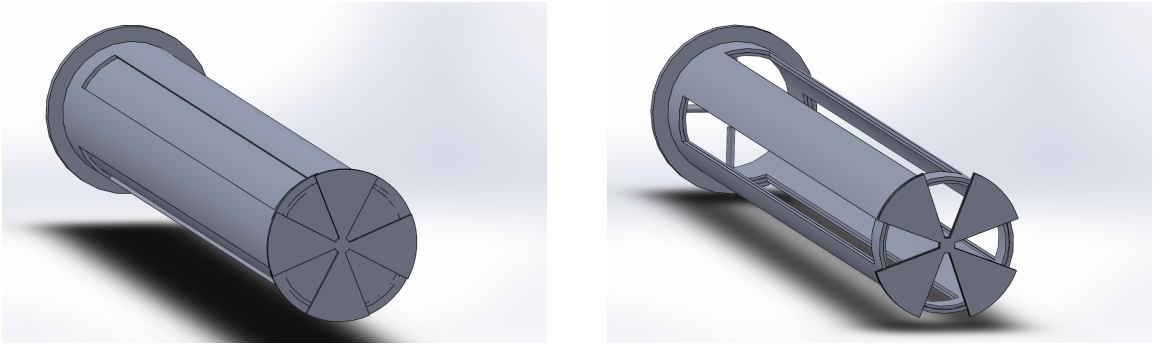

(a) Separator pipe closed (b) Separator pipe open

Figure 14: Separator pipe to restrict heat flow to the heat pipe

This new solution could make it so that the functionality of the old valve could be kept, while removing the disadvantages of having this part.

3.3.2 Modified plate

The plate from the original system, has a plate with a smaller diameter than the outer tank. The resulting gap between the plate and outer barrel is prone to heat losses. This gap also lets vapor from the oil in the system escape, resulting in a worse indoor climate, as well as diminishing oil level.

A new modified plate has therefore been modeled, this can be seen in Figure 13. To have a sealed off system, the plate needs to lie on the outer tank, which puts constraints on the size of the valve from the first system. With the valve replacement discussed in 3.3.1, this will not be a problem as the ball valve is removed. Unfortunately the plate was not made in time for it to be tested for this thesis, although it should be tested for further work.

3.3.3 Modified heating element

Due to a high temperature in the system combined with the location for the housing of the coupling box of the heating element, there was complications where the coupling box melted (see fig. 15). To reduce the resulting fire hazard, a new box was made from steel, and a high temperature cable was used.

The new metal housing can be seen in Figure 16, and is expected to have a much longer lifespan, than the original housing.

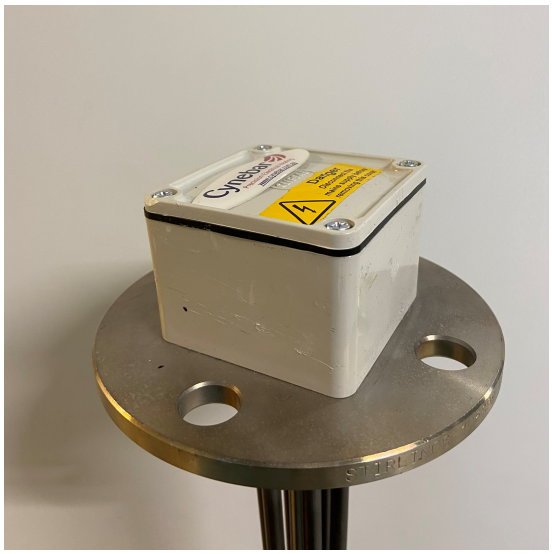

(a) Housing before melting

(b) Melted housing

Figure 15: Before and after pictures of the heating element housing

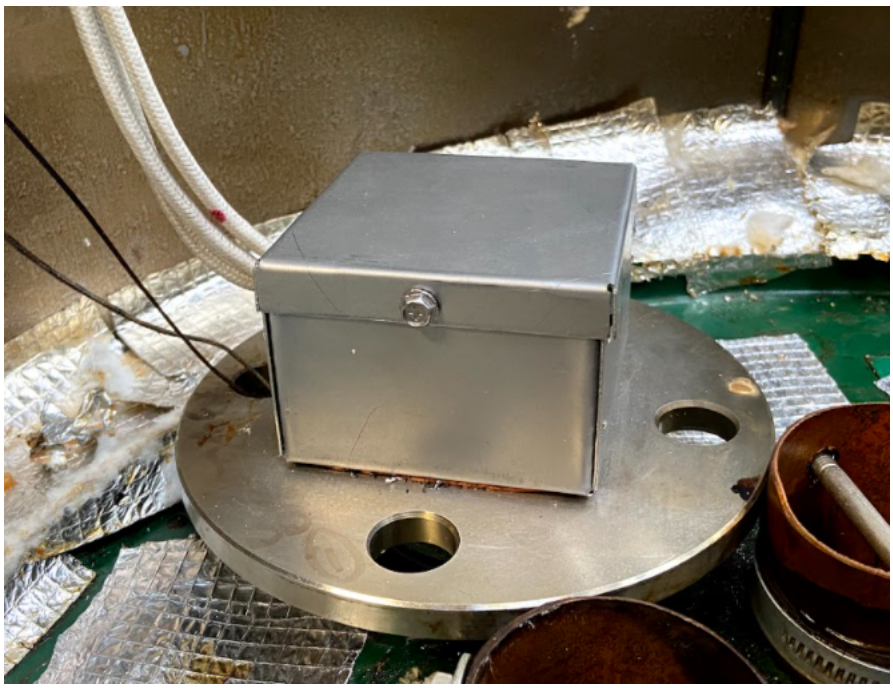

Figure 16: The new metal housing for the heating element

4 Numerical approach

A numerical model of the system has been made, to get insight in how the system behaves, as well as being able to simulate future modifications made to the system.

4.1 Numerical setup

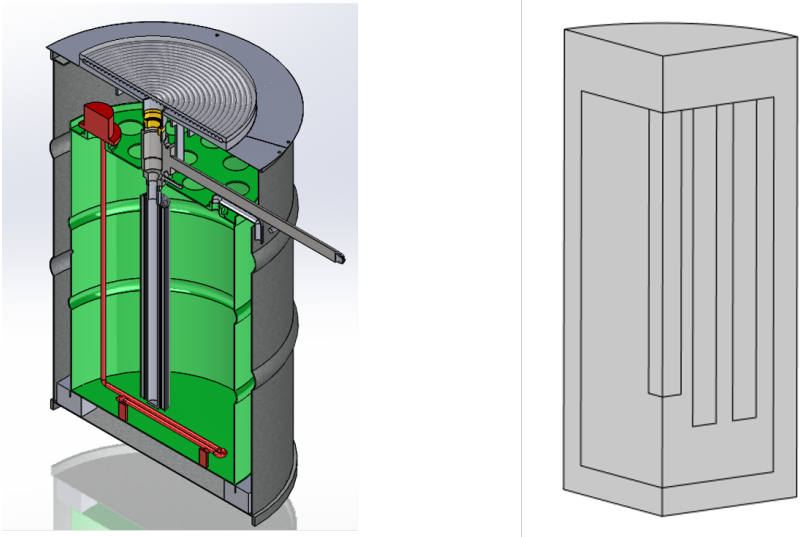

Figure 17: Comparison of the built system and the simplified numerical model

Numerical simulations of the system, was carried out during project work in the fall of 2020[10]. The numerical results gathered from this report will be compared to experimental results in Section 7.3.

4.2 Numerical aide for modified plate

Due to the new modified plate being larger than the previous model, the pressure forces on the inside will be higher. To test the geometrical constraints of the new plate, a model was made to test different thickness and pressure parameters. The thickness of the plate would need to be as thin as possible to reduce material use and thermal losses, while keeping its structural integrity during use.

To simulate the pressure forces in the plate a *solid mechanics* physics model was used[6]. Using this model, with inner and outer pressure boundary conditions on the plate set to 3bar and 1atm respectively, produced Figures 18 and 19.

Using information these figures, it was decided that the bottom plate would have to be 4.5mm. The top plate thickness was set to 1.2cm.

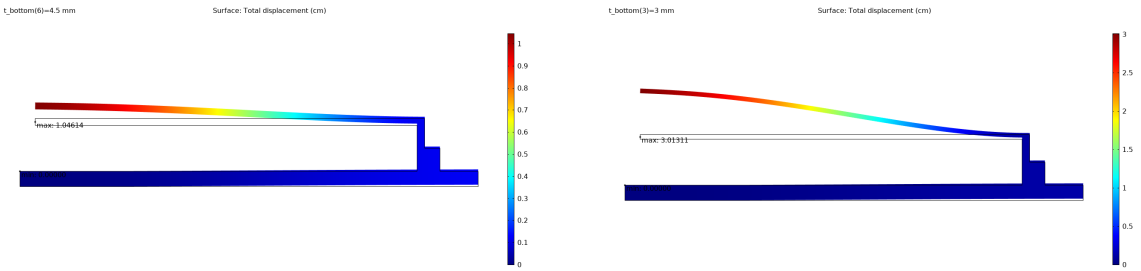

(a) Deflection with 3mm bottom plate (b) Deflection with 4.5mm bottom plate

Figure 18: Deflection of bottom plate using different thicknesses, $P_{in} = 3[bar]$

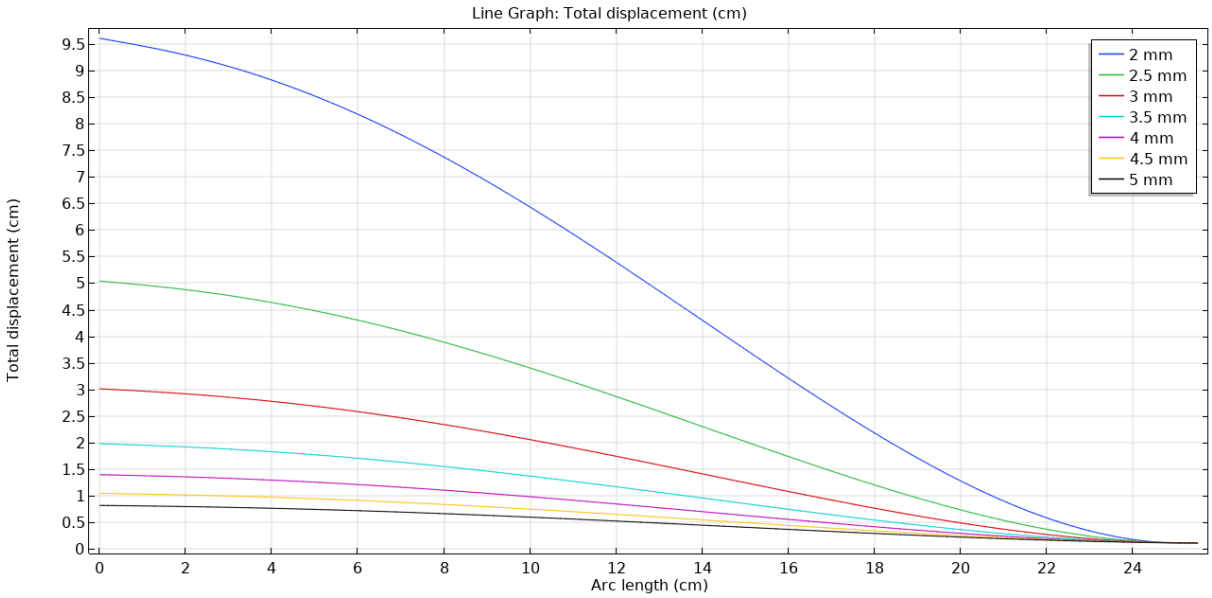

Figure 19: Total displacement of bottom plate using different thicknesses

5 Testing

The testing of the system, has been conducted using different test setups listed below.

1. Heating test
2. Discharging test
3. Frying test
4. Solar powered heating
5. Tests of modified system

The results of the tests are presented, and commented in Section 6.

5.1 Heating tests

In the heating tests, the system has been heated from ambient conditions to around 220°C. This final temperature was chosen because it is the melting temperature of the PCM. Operating in this temperature range, made it so that it should be possible to store latent heat in the system, in addition to sensible heat.

The goal of the heating tests, is to get an understanding of how long it takes to heat the tank, heat losses during heating, as well as looking at the temperature distribution within the system.

To reduce the heat losses from the system, and thereby reduce the total heating time, insulation has been put on top of the cooking plate. This insulation can be seen in Figure 20. Insulation on the underside of the plate was also introduced. The effect of this insulation will be presented in Section 7.

In the heating tests of the original system, the voltage used on the heating element was set to 220V. This was regulated by a voltage controller available in the lab, shown in Figure 21. With the given voltage and heating element, the output effect on the heating element, was approximately 1700W.

The tests conducted on the original system are listed below:

1. Ball valve open
2. Ball valve closed

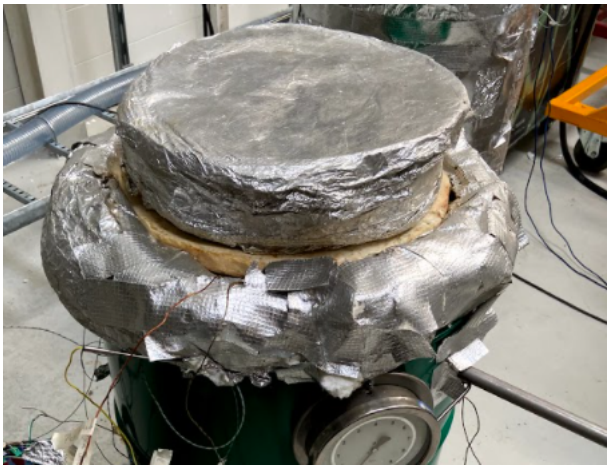

Figure 20: Insulation on top of the cooking plate

Figure 21: Picture of the controller to adjust the voltage

5.2 Discharging tests

The discharging tests, are the continuations of the heating tests explained in Section 5.1. After the system was heated to its final temperature, the heating element was switched off. This way it was possible to see the temperature decay of the system. The results from these tests, will be an indicator of how well the system contains heat and whether or not it will be suitable as a heat storage under the planned working conditions.

In the plots in Section 6.1, the test showing the temperature decay compared to the ones showing temperature development in the heating phase contains two more lines. These

Figure 22: Pot of water used in discharging experiment

lines represents the temperature of water in a pot. This pot of water, was placed on top of the cooking plate after the system had reached its maximum temperature. This pot can be seen in Figure 22. This setup was used to see how well the heat transfer from the tank to the cooking plate was. If the temperature decay in the plate is too great when in use, it will not be suitable for food preparation. To reduce the heat losses, simplify the heat transfer calculation and increase heat transfer to the pot, the pot was covered with a 5cm insulation layer after being placed on the cooking plate.

5.3 Frying test

As the system is intended to be used as a cooking top, the frying capabilities of the system has been tested. In this test, the system was heated close to its maximum operating temperature, before insulation of the plate was removed. After this, baking paper was put on top of the plate, and batter was placed on top. This tests is similar to the discharging test with a cooking pot, however the top was not insulated for this test, which might result in a higher heat loss from the plate.

Figure 23: PV panels used for solar testing in this report

5.4 Heating tests solar panels

To simulate the operating conditions of using renewable energy to charge the system, there has been performed tests using solar panels mounted at NTNU to provide energy to the system. The solar panels can be seen in Figure 23. These tests were performed from May 25th to May 28th 2021. The solar conditions were varying, and the power and solar radiation will be presented in Section 6.2. The solar panels used for the experiments performed in this thesis, are coupled in series, which leads to a higher output voltage[5].

5.5 Test of modified system

Modifications mentioned in Section 3.3 have also been tested, to see the effectiveness of the modifications made. The tests performed in this section, were carried out like the

tests listed in section 5.1.

The tests performed are listed below:

1. Valve replacement fully open
2. Valve replacement fully closed
3. Test of modified heating element housing

Testing the valve replacement fully open, is to see if it has a too high impact on the heat transfer. If this was the case, the system would not work in the open state, and another solution would have to be found. Testing the valve replacement closed, is to see whether or not the replacement works as inteded, restricting heat transfer when closed.

6 Test results

6.1 Heating and Discharging results

The results in this section, is acquired using the test setup explained in Section 5.1.

6.1.1 Original system, ball valve open

Heating
Figure 24, shows the temperature development in the original system in the heating phase, with the ball valve open.

In Figure 25, one can see the temperature plotted with the pressure inside the plate and heat pipe. The pressure inside the plate, is monitored to make sure that it does not exceed the threshold set for the relevant plate. For the original plate used in this testing, the pressure threshold is set to 3 bar. From Figure 25, it is therefore clear to see that the pressure does not exceed the threshold, and that it is well within the set operating range.

Looking at Figure 25, one can also note that the temperature of *Plate Middle*, has a temperature drop that *Plate Radius* does not. This is due to the pot of water in this test being placed on top of the thermocouple logging *Plate Middle*.

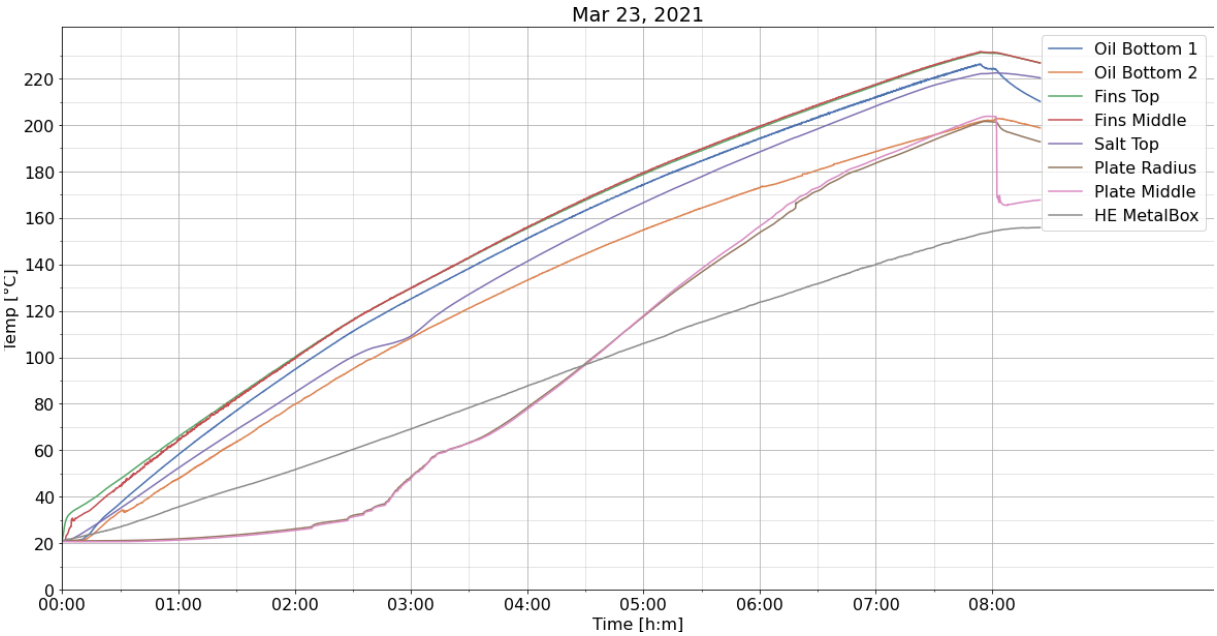

Figure 24: Heating test original system, heating element connected to power grid, open valve

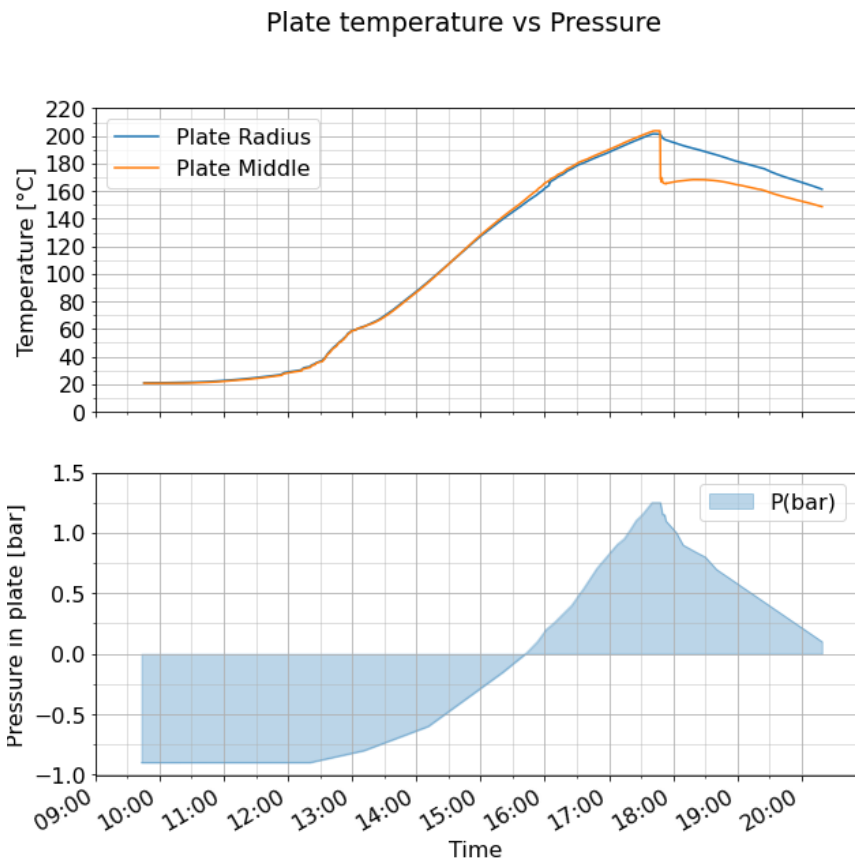

Figure 25: Pressure development in the plate and heat pipe compared to the temperature in the plate, original system, open valve

Discharging

Figure 26 shows the temperature decay of the system after the heating element is switched off.

The lowermost lines in the plot, shows the temperature development in the water. It shows that the water reaches a temperature of 100°C, and that the system keeps the water at boiling temperature for about 3 hours.

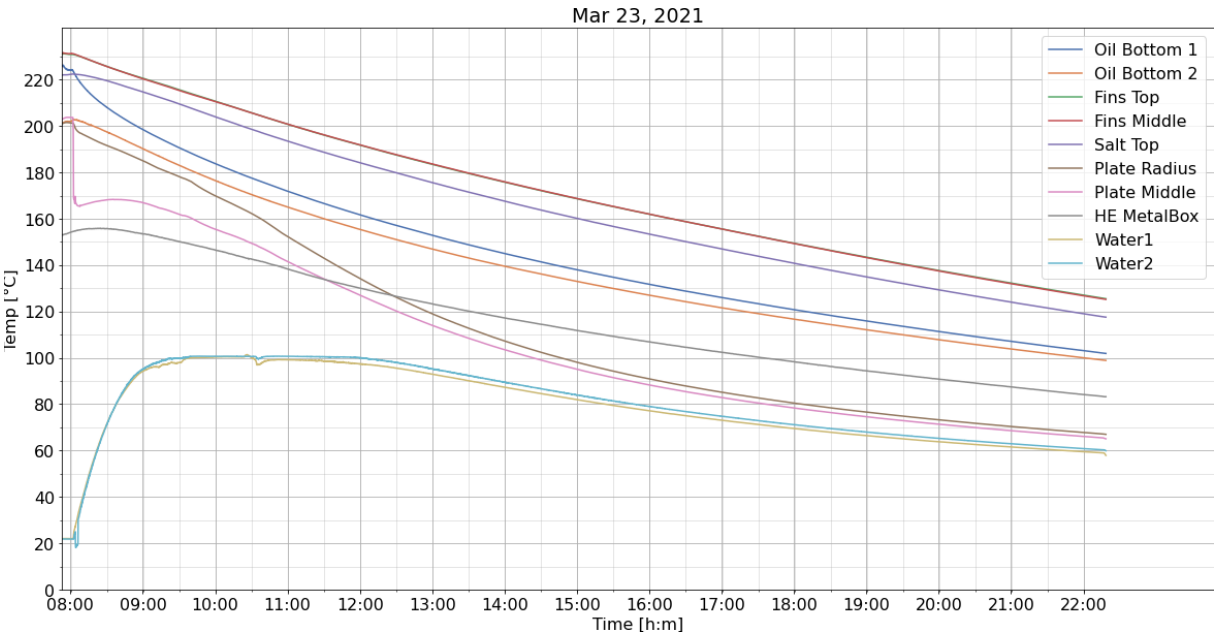

Figure 26: Discharging phase of original system, open valve

6.1.2 Original system, ball valve closed

The test setup used in this section, is identical in the heating phase to the one presented in Section 6.1.1, apart from the ball valve being in the closed position for this test.

The goal for this test, was to see how well the valve restricted the heat flow from the storage to the plate. This would give an indication as to whether or not the system can be cooled by closing the valve. The test will also give insight into how fast the plate heats after opening the valve. If the heating response in the plate after opening the valve is slow, this would have to be taken into account.

Heating

Figure 27 shows the temperature development in the system when the ball valve is in the closed position. Compared to the test shown in Section 6.1.1, it is clear to see that the temperature development in the plate is far slower, than that of the test with the valve open.

After about 5 hours of heating, the temperature in the plate increases drastically. This is due to the valve being opened, and the propylene glycol vapor being able to freely reach the underside of the plate.

Discharging

The discharging plot shown in Figure 28, is the continuation of the heating plot from Figure 27. The valve was closed right after the system reached its maximum temperature, as indicated in Table 7.

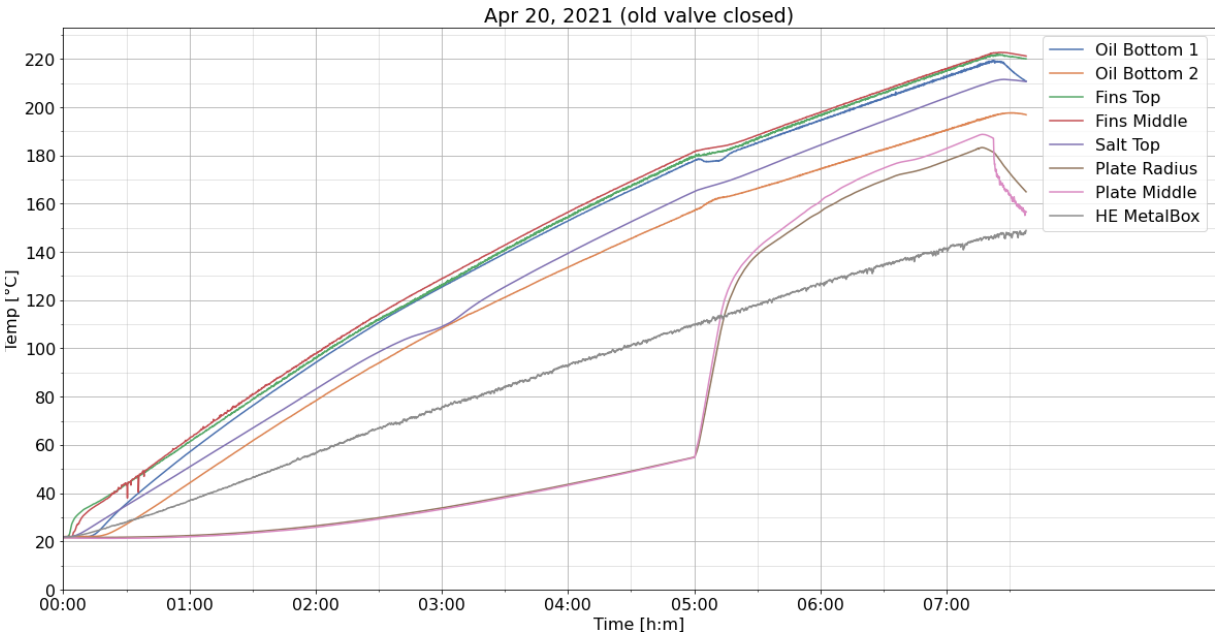

Figure 27: Heating test original system, valve position as explained in Table 7

time of day/ from start	Note	Heating element voltage
08:30 / 00:00	Startet experiment, valve closed	220V
13:30 / 05:00	Opened valve	220V
15:42 / 07:12	Closed valve	220V
15:50 / 07:20	Reduced voltage	160V
15:51 / 07:21	Took off inner insulation on plate	160V
15:55 / 07:25	Turned off heating element	0V

Table 7: Notes taken from experiment, original system, closed and open valve

After closing the valve, the pressure was carefully monitored to make sure it did not exceed the threshold that was set for the current plate. The pressure in the heat pipe plotted with the temperature can be seen in Figure 29.

The difference between having the valve open and closed in the discharging phase can be seen in Figure 30. To make sure that this is not the entire system cooling down faster due to less insulation, the temperature decay of Fins Middle and Fins Top can be seen in Figure 31.

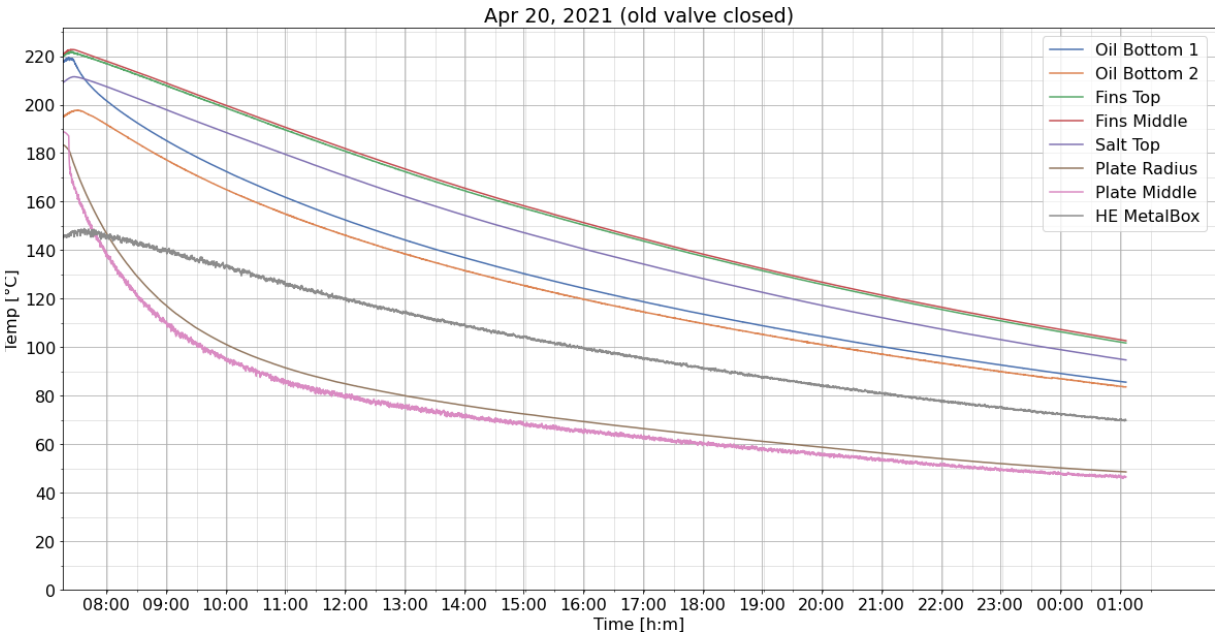

Figure 28: Temperature development in discharging phase with closed valve

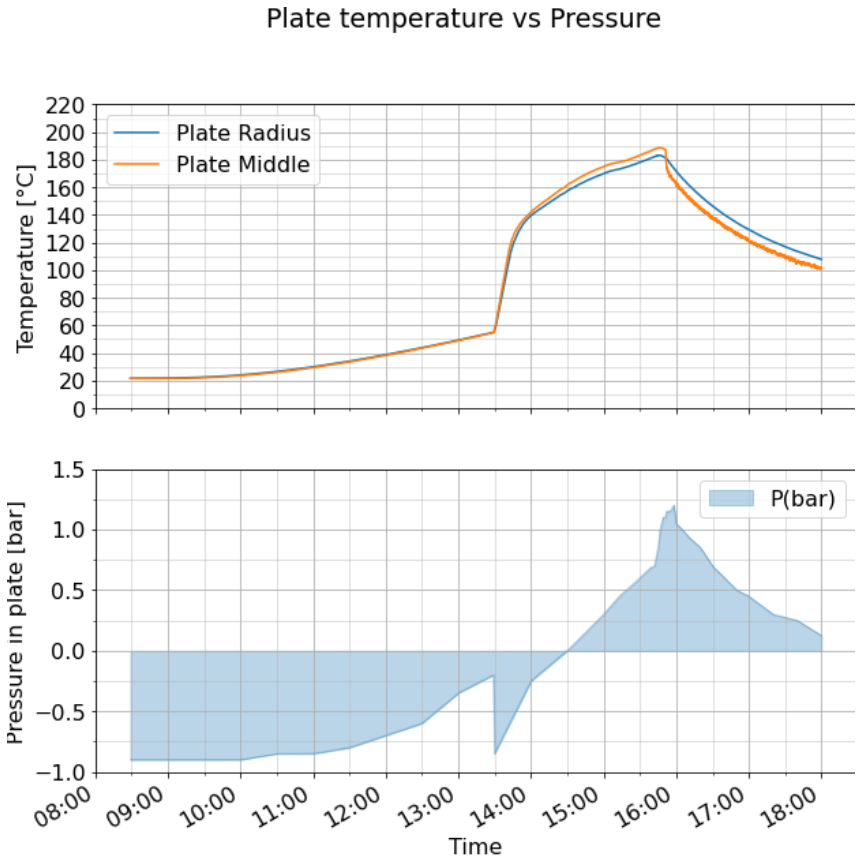

Figure 29: Pressure development in the plate and heat pipe compared to the temperature in the plate, valve position explained in Table 7

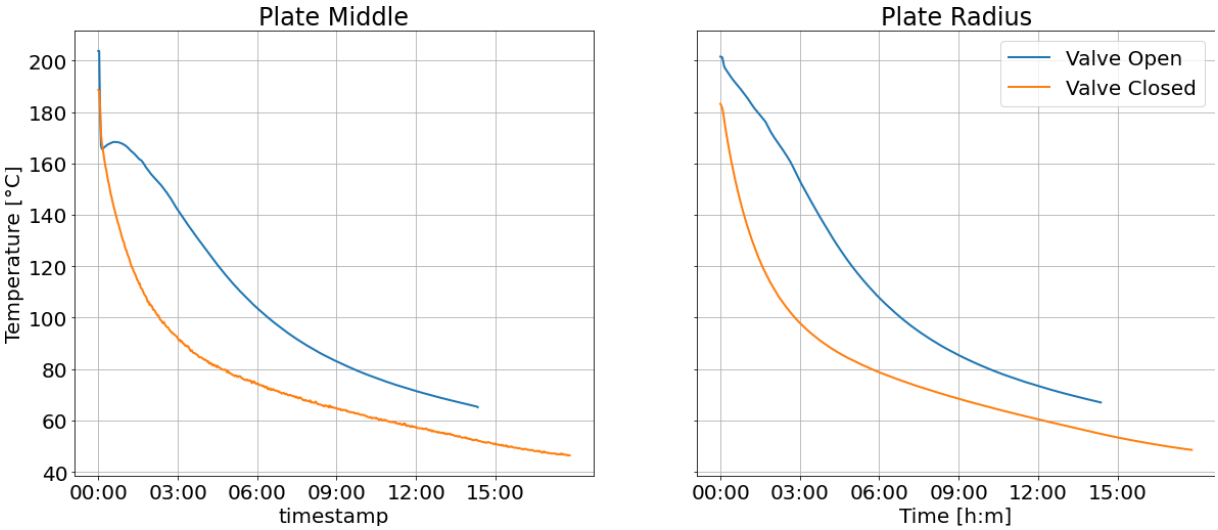

Figure 30: Comparing the temperature decay of plate with open and closed valve

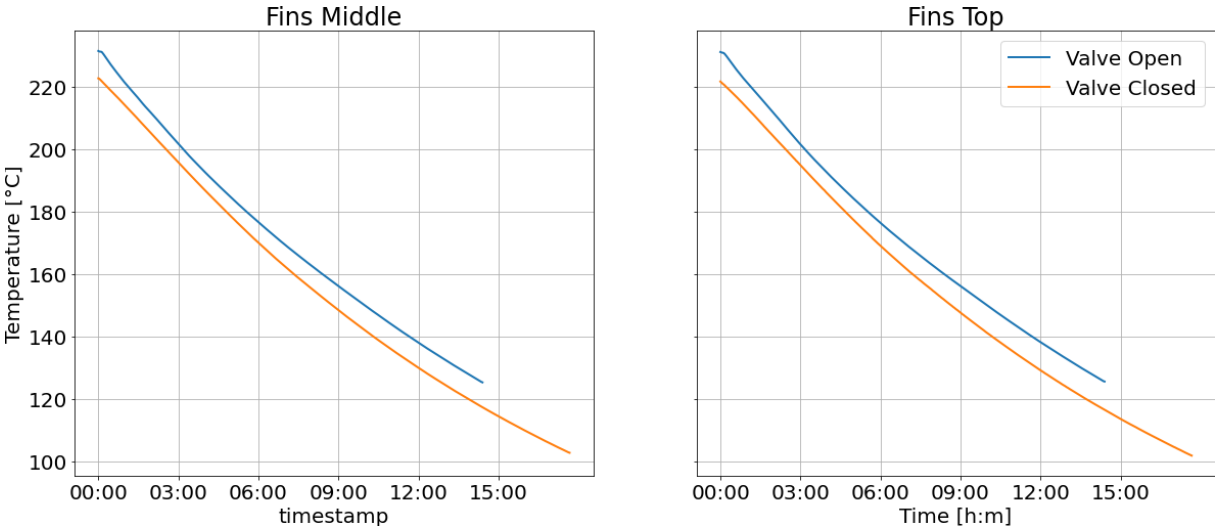

Figure 31: Comparison of temperature decay close to heat pipe with open and closed valve

(a) Crêpe in the making (b) Resulting crêpe from frying test

Figure 32: One crêpe made during frying test

6.1.3 Frying test

In the frying test, the system was heated to operating conditions using the power grid and 220V on the heating element. During the actual frying, the temperature of the system was kept close to constant by adjusting the heating element voltage back and forth in the range 140V-160V.

Figure 32, shows the making, and result for a crêpe made during this test. The temperature plot from the frying test can be seen in Figure 33, with the corresponding events in Table 8.

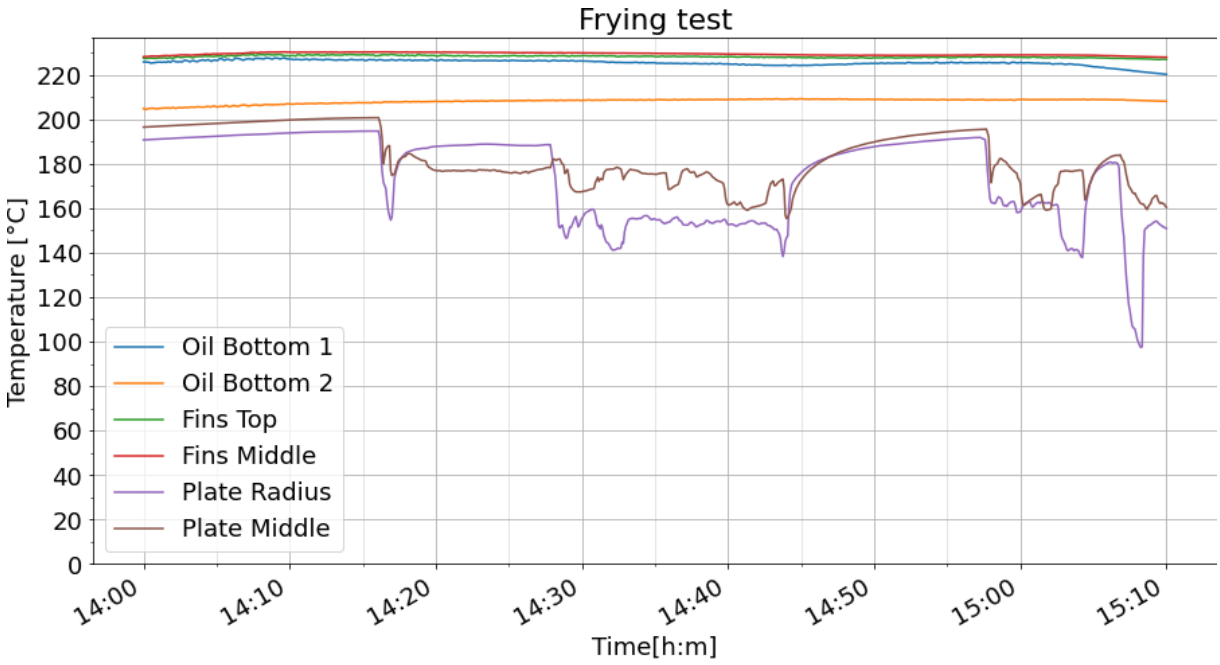

Figure 33: Temperature in system during frying test

Timstamp	Note
14:16	Removed inner insulation from plate
14:17	1st batter on plate(crepe)
14:25	Crepe (1st test) finished
14:27	Removed outer insulation from plate
14:33	2nd batter on plate(injera)
14:36	Put lid over injera batter
14:37	Injera (2nd test) finished
14:39	3rd batter (injera) on plate
14:43	Injera (3rd test) finished
14:44	Put insulation back on plate
14:57	Removed insulation from plate
14:58	4th batter (injera) on plate
15:03	Injera (4th test) finished
15:04	Turned off heating element
15:06	Removed all insulation from plate and closed valve
15:07	Used a fan to try to cool the plate
Onwards	Tried blowing wind on the plate using a lid to cool the plate

Table 8: Notes taken from frying test

Figure 34 shows the temperature heating of the tank from around 90°C. The figure shows that the thermocouple logging *Fins Top* reaches a temperature of 220°C after 5 hours of heating from 100°C.

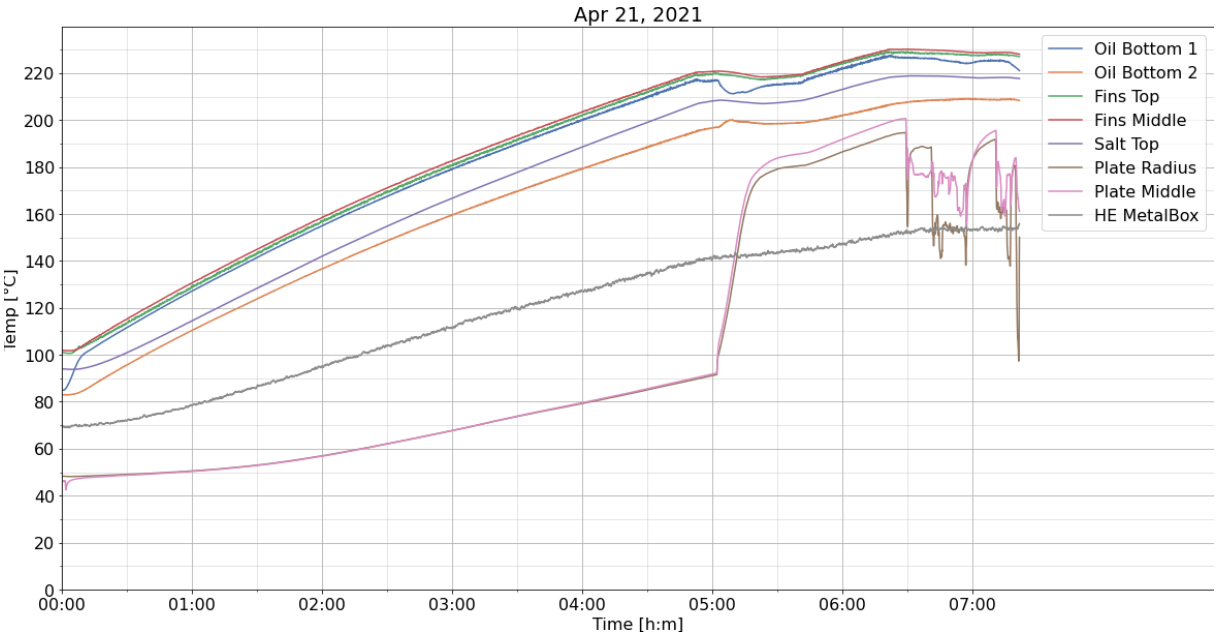

Figure 34: Heating time for frying test

6.2 Heating solar panels

The results in this section is acquired by using the test setup described in Section 5.4.

6.2.1 Test 1

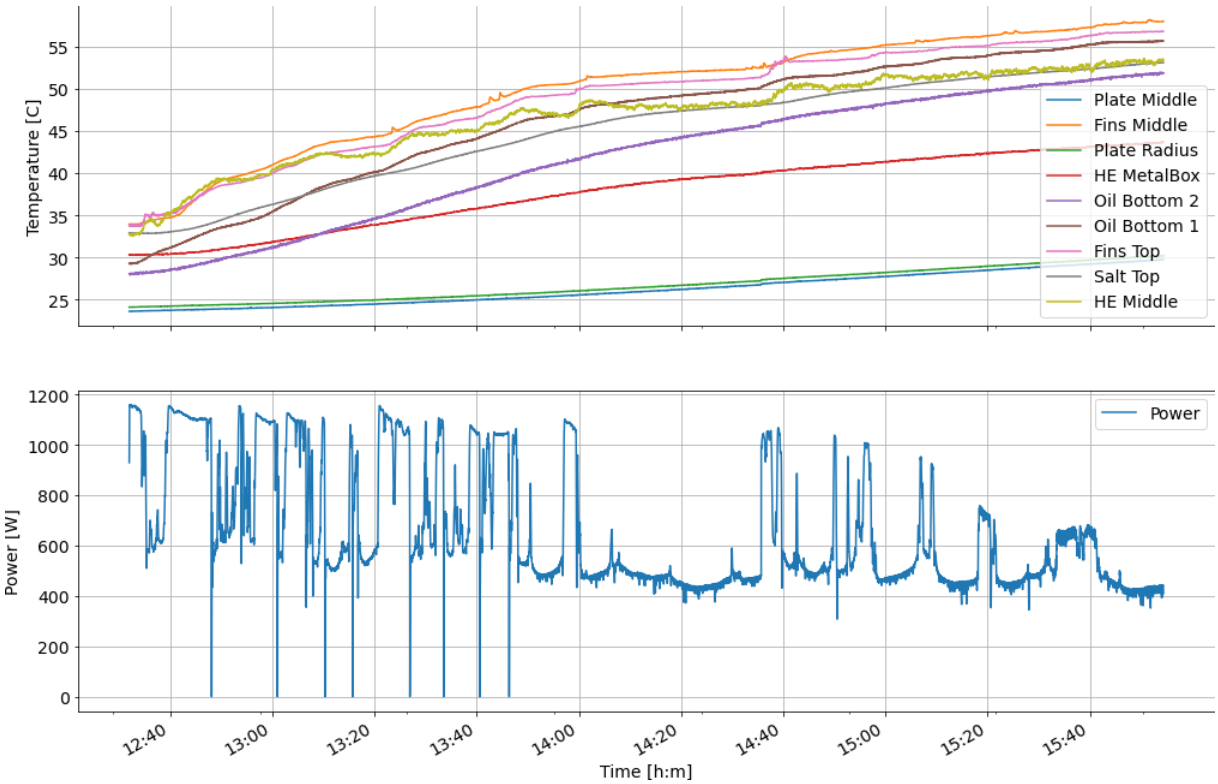

Figure 35: Test 1 using solar power

The first test, was postponed due to grounding problems mentioned in Section 6.2.5. The test is therefore a lot shorter than the other tests performed in this section, and the overall temperature increase was only 60°C after 3 hours. In addition to the heating time being shortened, Figure 35 shows that the solar conditions also was a limiting factor.

6.2.2 Test 2

The temperature development for the second test as well as the heating element power, can be seen in Figure 36. The figure shows that the maximum temperature reached was around 105°C, around 100°C lower than the temperature acquired after the same amount of heating using the power grid.

The slow heating is partially due to the solar conditions being limited due to cloudy weather.

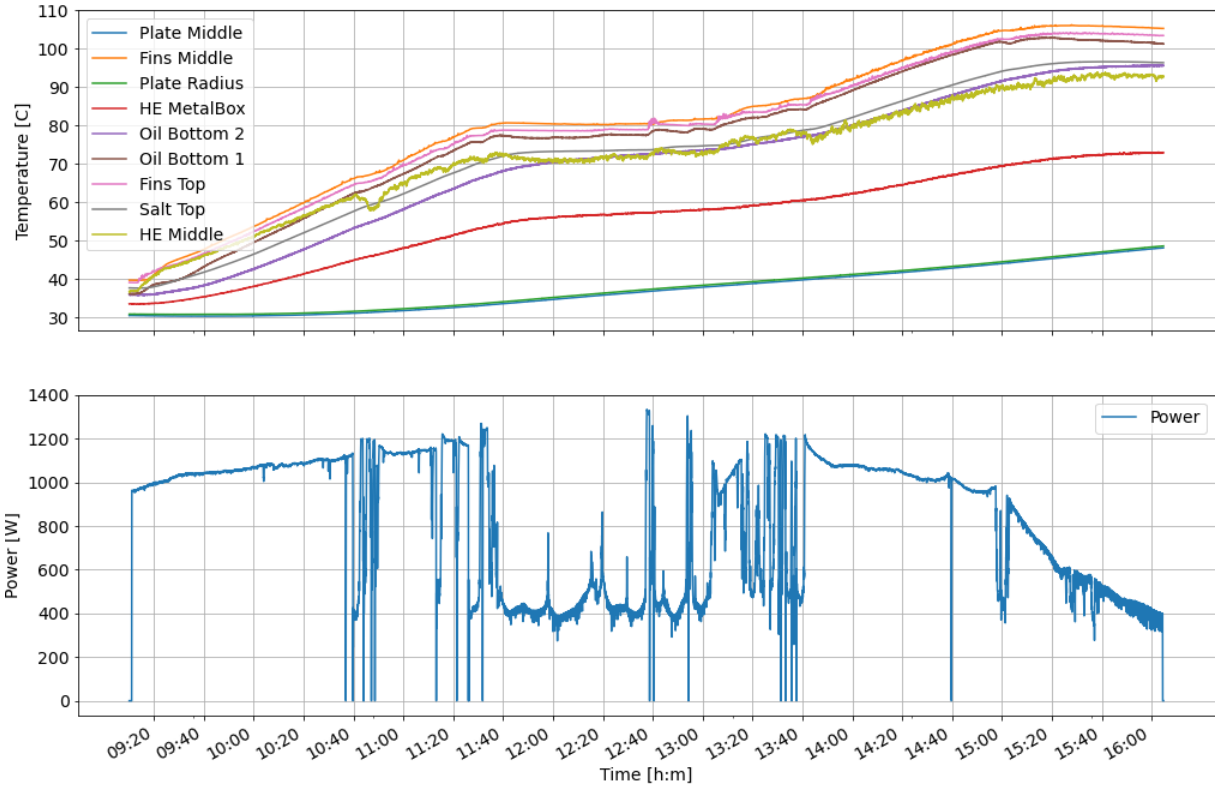

Figure 36: Test 2 using solar power

6.2.3 Test 3

During the third test using solar panels, the solar conditions were far better than the day before. This can be seen in Figure 37. Better solar conditions combined with a higher starting temperature, resulted in the maximum temperature of this test to be 130°C after 6 hours of heating.

6.2.4 Test 4

Figure 38 shows the temperature development for the fourth test using solar panels. With a starting mean oil temperature of around 65°C, it had the highest starting point of the four tests. However, due to poor solar conditions, the maximum temperature of the test did not exceed 125°C. This is less than the day before, that had a lower starting temperature.

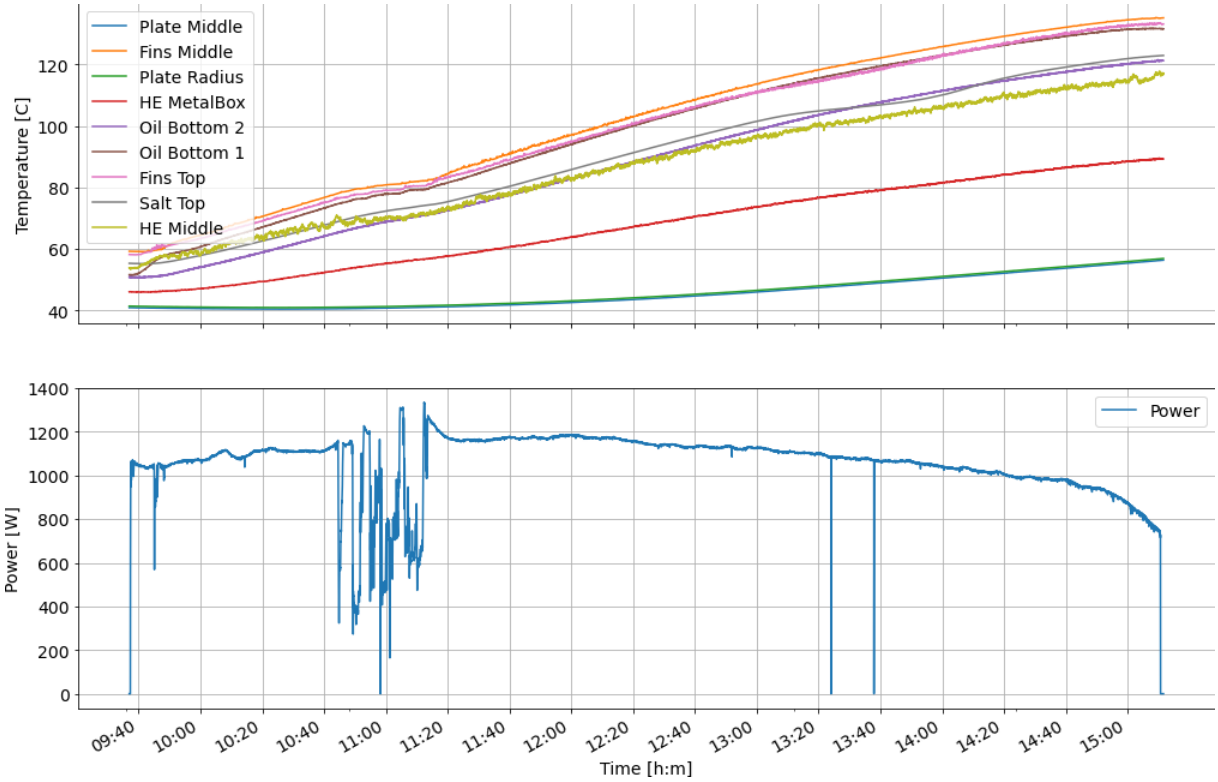

Figure 37: Test 3 using solar power

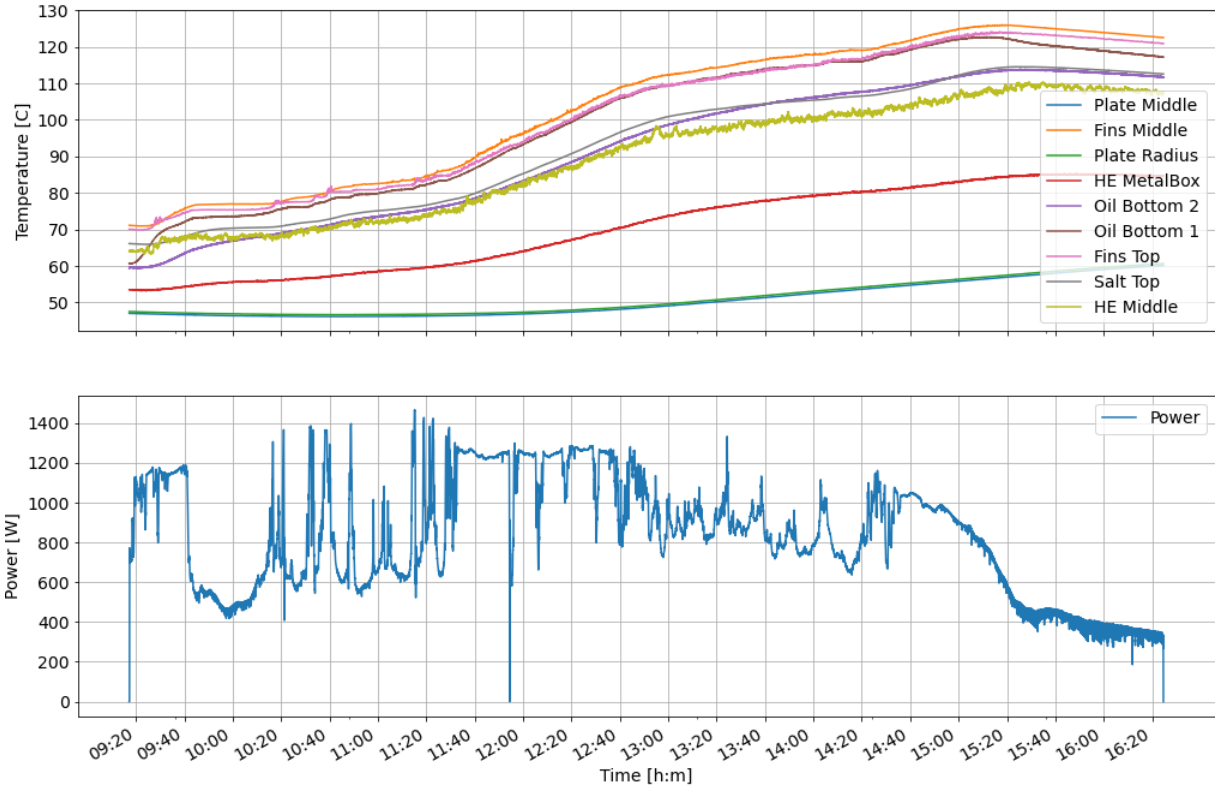

Figure 38: Test 4 using solar power

6.2.5 Grounding problems

When it was time to test the solar panels, the system had a grounding malfunction. This led to electrical noise in the measuring devices and resulted in wrong temperature readings shown in Figure 39. By connecting some metal between the system and ground, it was possible to remove the problem, and the system worked as intended. The permanent solution, was to ground the power cable coming from the solar panels.

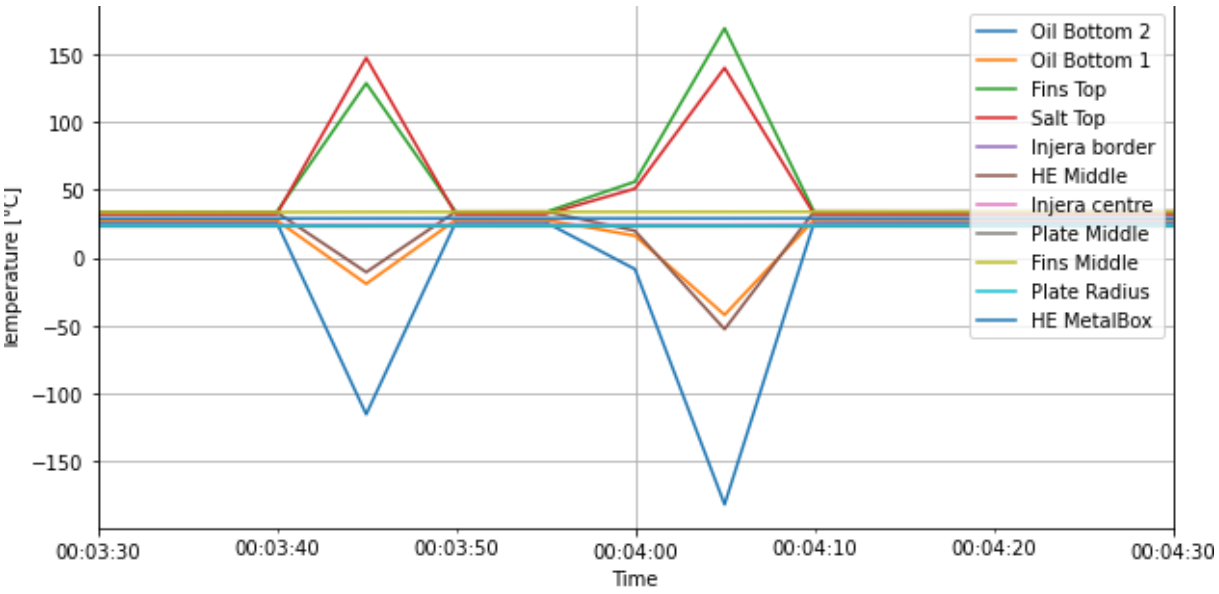

Figure 39: Temperature readings with grounding problems

6.2.6 Solar conditions

The solar conditions during the days of testing, are presented in Figures 40 and 41, showing the solar radiation and the power given to the heating element. The solar radiation is monitored using a sensor independent of the solar panels, therefore the plot showing the heating element power, drops more than the solar radiation towards the end of the tests.

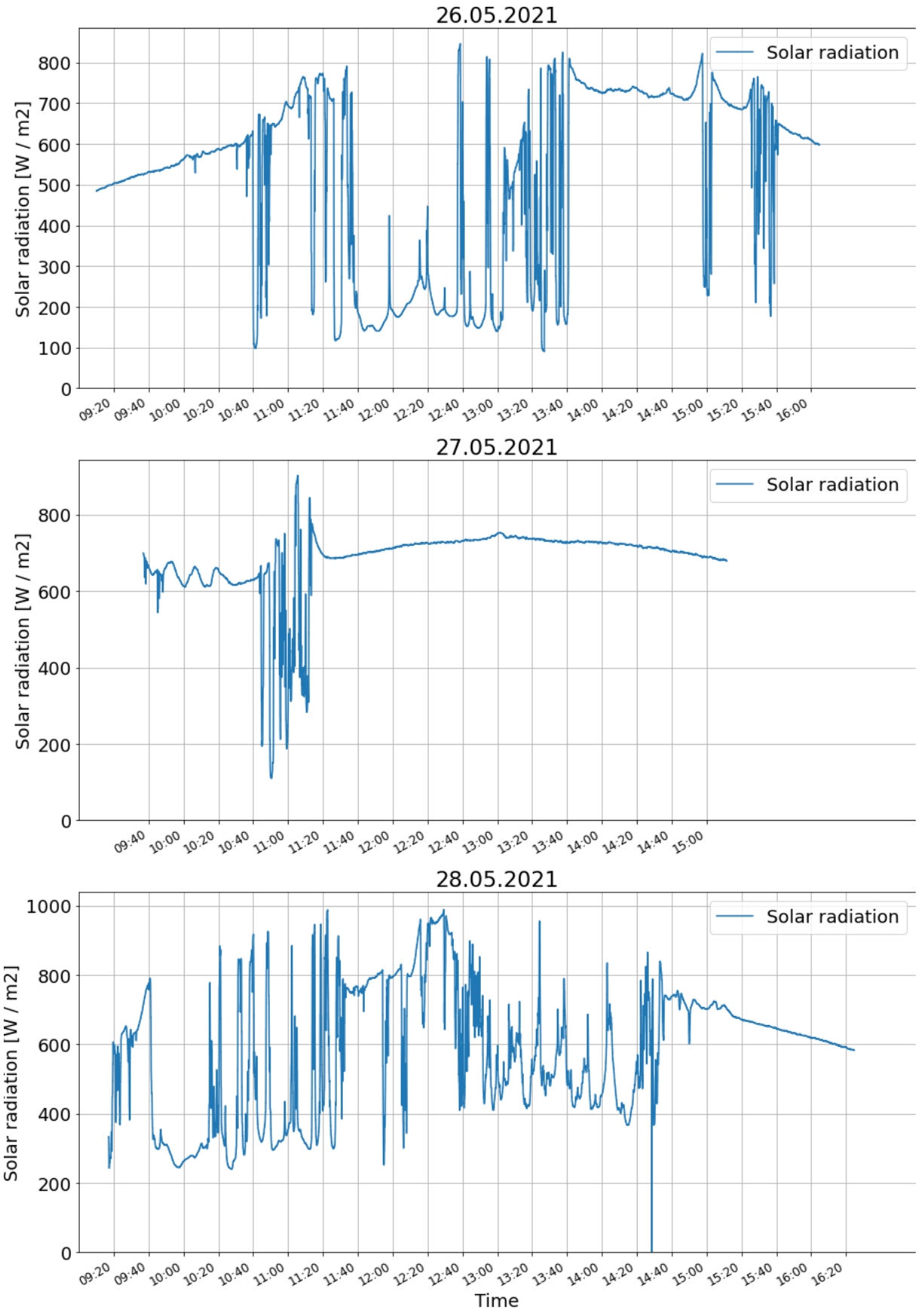

Figure 40: Solar radiation measured on the days of solar testing

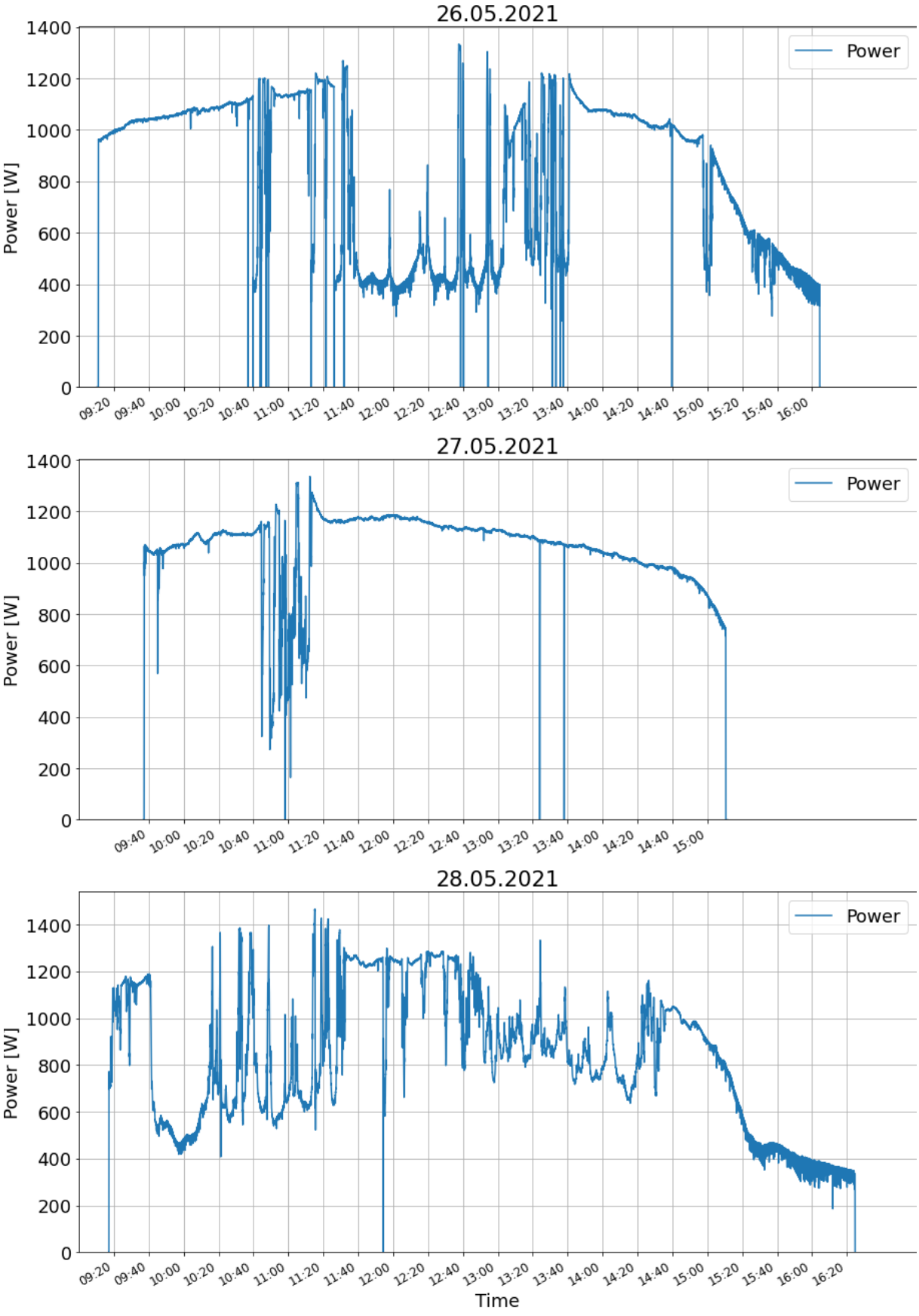

Figure 41: Power provided from solar panels measured on the days of solar testing

6.3 Modified system results

6.3.1 Valve replacement

Figure 42, shows the temperature development in the system while using the new valve replacement in the open position. From the figure, one can see that the temperature development in the tank, does not seem to be heavily restricted, implying that the valve replacement does not reduce the heat transfer when in the open position.

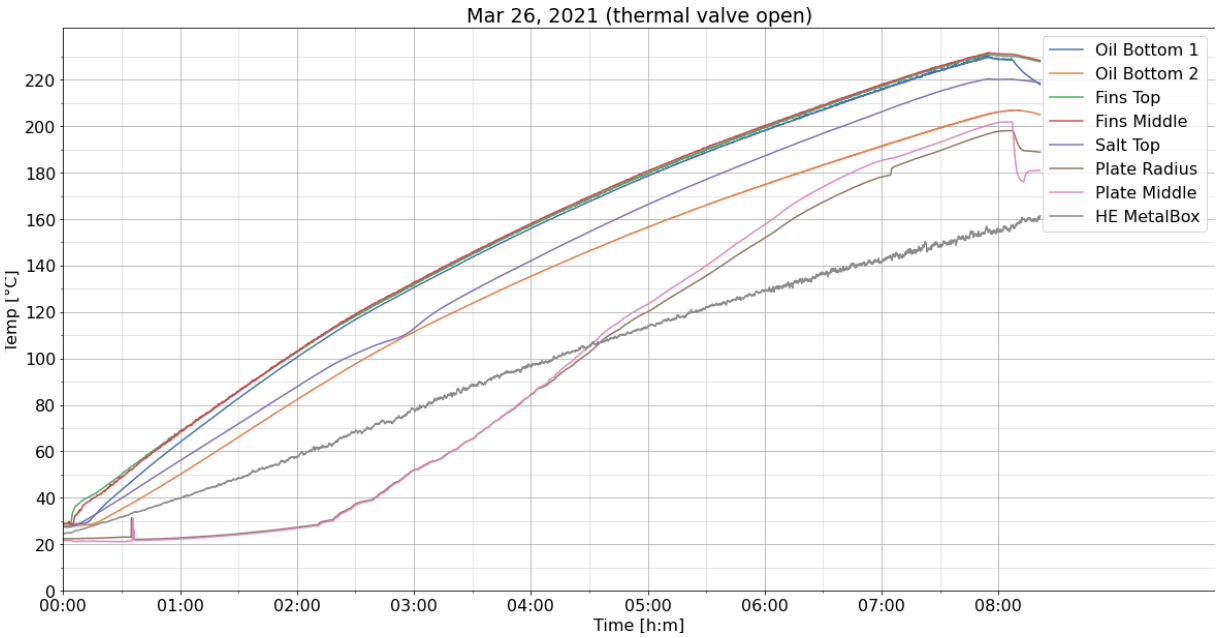

Figure 42: Heating test with thermal valve open, connected to power grid

Figure 43 shows the temperature development in the system using the valve replacement in the closed position. Looking at the graph, it can seem as if the temperature in the plate remains unaffected in terms of heat transfer. To compare the four different valve configurations, Figure 44 shows the temperature development in the plate using the configurations; ball valve open, ball valve closed, valve replacement open and valve replacement fully closed. This figure shows that the plate temperature almost coincides for the base test, open thermal valve and closed thermal valve.

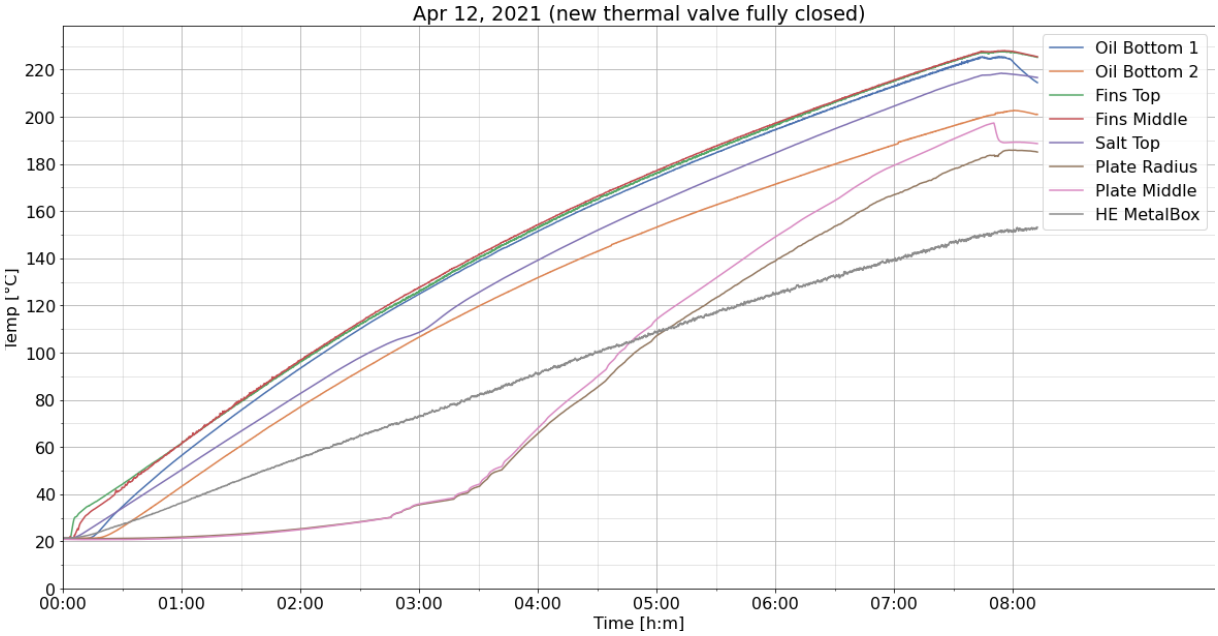

Figure 43: Heating test with thermal valve closed, connected to power grid

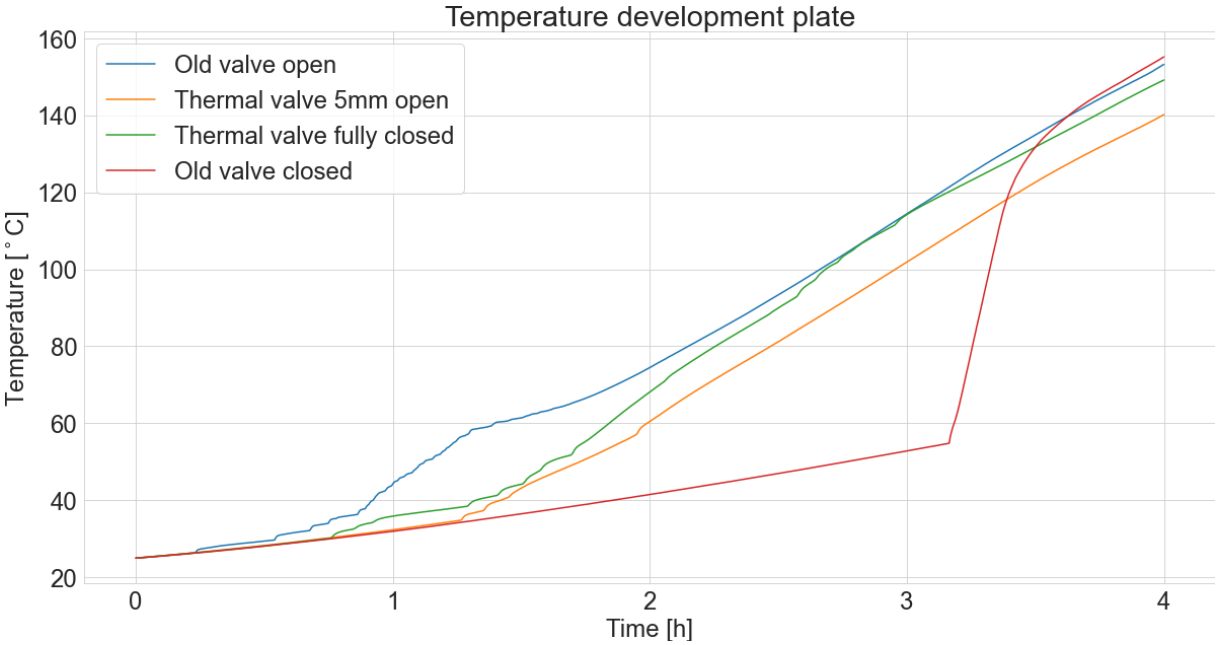

Figure 44: Temperature development of four different valve configurations

7 Discussion

7.1 Original system

7.1.1 Heating time and temperature decay

The heating test with the ball valve open, can be regarded as the base test for the system. All modifications made to the system, as well as other tests performed this spring, revolves around this base configuration working as intended. From results gathered in Section 6.1, it looks like the system can be used as an effective heat storage.

Looking at figures shown in Section 6.1.1, one can note that the total heating time is rather high. From Figure 24, one can see that the total heating time is about 8 hours. During regular use, the heating time should be shortened, as the starting temperature of the tank will be a lot higher due to it being heated on a daily basis. Therefore this prolonged heating is a one time case, and should not be an issue in daily use.

Figure 28, shows that the bulk temperature in the oil is around 90°C after a temperature decay over 17 hours starting at 220°C. This is the starting temperature of the heating plot shown in Figure 34, which shows that the system reaches a temperature of 220°C after just 5 hours. This is a great decrease in time from the 8 hours used to heat the system from ambient conditions. Here it is also worth noting that the temperature decay in Figure 28 represents a system where the top insulation is removed, to make the plate temperature decrease faster. Therefore it is plausible that the final temperature after the discharging period would be higher, if the system had been fully insulated.

Another factor that might affect the temperature decay of the system is that the system only contains 6 out of the possible 16 PCM cylinders. Increasing the amount of PCM cylinders in the system should increase the storing capacity of the system in the working temperature range, and thereby decrease the temperature decay. Looking at Table 4 from Section 2, one can see that the heat storage can store around 16% more energy with 18 PCM cylinders compared to 6, in the relevant temperature range.

One more thing to note from the heating tests, is that some of the HTF evaporated during the heating tests. This resulted in fumes leaking out of the tank. Due to the oil being non toxic it is not a health issue, however it needs to be addressed, as it decreases the quality of the indoor climate, as well as resulting in a diminishing oil level over time. Therefore it would be of interest to create a way of recovering these gasses.

7.1.2 Solar heating

From Figures in Section 5.4 one can see that the heating was greatly affected by solar conditions. During tests using solar panels as the source of power, the maximum temper-

ature of the tank was around 140°C. With an effect of maximum 1200W on the heating element, the system will with today's setup require several days of heating to reach the operating conditions.As touched upon in Section 2 however, the amount of energy stored in the system using PCM, is greatly increased if the system exceeds the PCMs melting point. Having a higher storing capacity at higher temperatures, the system might benefit from having a higher starting temperature utilizing solar power for heating.

To accommodate for the solar conditions in Trondheim. It might be of interest to install more solar panels, or change the location that is set today. The solar panels are today mounted on a roof around several other installations that can cast a shadow on the panels. This would reduce the effectiveness of the panels throughout the day. Due to the panels being mounted in series, which is necessary to have a high voltage output, the system relies on all panels having good solar conditions[5]. Therefore it might be of interest to move the panels to a location that is less prone to shadows.

When it comes to the use of solar energy in sub-Saharn Africa, one can look at the solar conditions in Addis Ababa, Ethiopia. The day length in Addis Ababa, Ethiopia, the day length ranges from 11 hour 36 minutes to 12 hours 39 minutes throughout the year[2]. By looking at the temperature decay in the system from Figure 28, the temperature goes from 220°C in the oil to 120°C over a time span of 13 hours. This temperature decay is also thought to be lowered with better insulation. The time it takes for the system to heat from this to the desired temperature, is around 4 hours. From this it should be reasonable to heat the tank to working conditions using solar power.

7.2 Modified valve comparison

A comparison of the different valve configurations is shown in Figure 44. In the four cases, the system has been heated with the heating element used for all tests with a voltage of 220V. In the figure, the valve replacement is denoted as *Thermal valve*. From the figure, one can see that the temperature development in the plate is slightly prolonged in the start phase of the heating. This is true for both the open and closed thermal valve. However, the restriction of heat transfer is negligible as the system is heated further. Resulting in the lines almost coinciding. Because the system is intended to store heat at a high temperature, the valve would need to be able to restrict heat while the tank is hot. From this test, it is clear that the modified valve does not fulfill this criteria.

From these results, one can say that for the temperature in the plate to be restricted, a new solution will have to be found. However it might be worth looking into making a system without a valve altogether. Removing the valve without making a replacement would result in a much more robust and cost efficient system. One drawback of building the system like this, is that you lose the ability to cool the plate between use. However looking at the results in Section 6.1.2, the temperature decay in the plate with the valve closed is still quite slow. This could imply that it is not the best solution to cool the plate in the first place.

After removing the valve, it will be of interest to look into insulating the top of the plate. This would serve two purposes; restrict heat losses and make the system safer with less exposed hot surfaces. To resolve the cleaning problem, one could use and extra layer to put on top of the plate, as was done in the frying test from Section 5.3. The layer used, would need to have a low thermal resistance, as it should not restrict the heat output from the plate.

7.3 Comparrison with numerical simulations

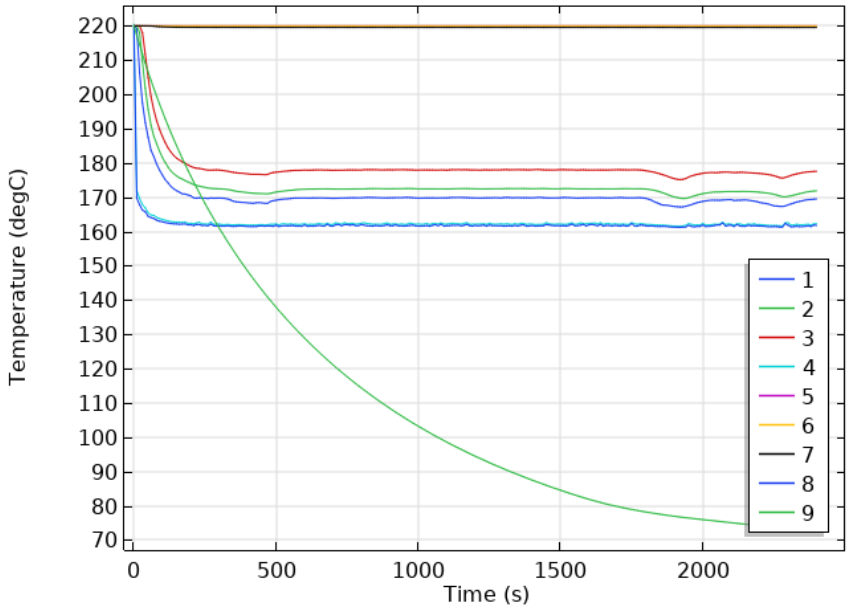

Figure 45: Temperature development with constant temperature boundary conditions, CFD simulation

Figure 45, shows the temperature decay found through numerical simulations, acquired through the project work for this project[10]. The numbered points in the graph is logged using the virtual thermocouples that are shown in Figure 46. From the figure it is clear to see that the temperature decay is happening far more rapid than the temperature decay of the experimental testing. This is due to the simulations using a constant temperature boundary condition on the PCM and heat pipe of 220°C and 160°C respectively.

Because the conditions for the simulations and the experimental work is so different it is hard to draw comparisons between them, however one can see that the temperature difference in the oil, does vary substantially in the vertical direction. This can be seen in both the experimental and numerical testing. Due to the system having a higher temperature in the top of the tank compared to the bottom, it seems as if the PCM will be heated from the top. This is of interest as it might result in the top part of the PCM melting first. If it was heated from the bottom, the PCM cylinders might experience a pressure buildup in the bottom, which could be a hazard.

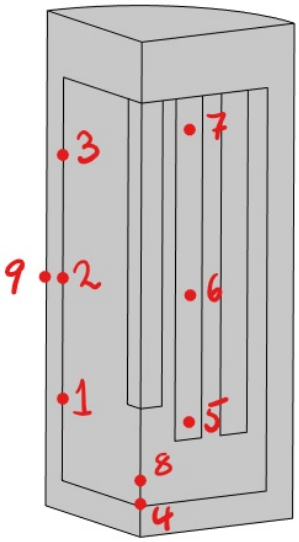

Figure 46: Position of virtual thermocouples used in CFD simulation

8 Conclusion

8.1 Heating

Tests presented in Section 6, shows promising results in terms of heating and energy retainment of the system. This implies that the system should be able to be used on a daily basis, if the system is regularly heated. Tests performed this spring shows that the temperature decay is acceptable, however, the tank should be insulated better for future versions, further improving the energy retainment.

8.2 Heat transfer plate

From tests presented in Section 5.2 and 5.3, the heat transfer from the system to the plate, as well as from plate to desired cooking pot or food is quite good. The system shows great potential in heating as well as maintaining a high temperature during use. The system was able to boil water for around 3 hours, which should make it viable for a frying cooking application.

8.3 Solar panel potential

The use of solar panels combined with this system is a possibility. Tests has shown that the system contains heat well enough for solar power in certain areas can be an effective way of heating. This however, requires solar panels with a higher effect than what was produced in tests in this project. This power requirement, might not be as strict, if heat losses from the tank are lowered even further, which can be done through better insulation.

The system might also have been capable of staying within operating conditions in the solar tests performed in this report, if the amount of PCM cylinders and starting temperature is increased.

8.4 Valve replacement

The valve replacement built for this project, did not work as intended. The effect of the separator pipe was insignificant, and the design was scrapped. However due to the original ball valve not having a great effect on the plate temperature in the first place, the valve will be removed completely. The new design will revolve around having proper insulation on the plate, and finding another way to keep the plate clean during and after use.

9 Further work

9.1 Solar tests

There should be carried out tests involving solar panels, where the starting temperature of the tank is higher than in the experiments performed in this project. From calculations and theory, the system can contain more energy at a higher temperature. Starting at a higher temperature might result in a lower temperature decay. For these tests the system can be preheated by the power grid to save time.

There should also be conducted tests using solar panels under the planned working conditions of the system. The solar conditions in Trondheim Norway does not reflect the conditions in sub-Saharan Africa.

9.2 Tests on modified system

The new plate that has been built, will have to be tested, to see how well it performs in terms of heat transfer, pressure buildup as well as comparing the total temperature decay of the system using this new plate.

There should also be conducted tests where more PCM cylinders are used. The tests performed up until now, gives an indication of the effect of PCM in the system, however it would be beneficial to see the effect of having more cylinders in the system. This is especially true in the high temperature regions.

9.3 Frying tests

To test the frying capabilities over a longer period of time, the frying test performed this semester should be up-scaled. The results from the test performed this semester is promising, however it would be beneficial to see the potential limitations the system has during use. This can be done by using the plate to make several consecutive injera.

9.4 Further modifications

To reduce the amount of fumes coming from the oil inside the tank, there should be made a way of recovering these gases. This would better the indoor climate, while at the same time potentially reducing heat losses.

References

[1] Access to electricity. https://www.iea.org/reports/sdg7-data-and-projections/access-to-electricity. Accessed: 2021-03-15.

[2] Addis Ababa, Ethiopia — Sunrise, Sunset, and Daylength. https://www.timeanddate.com/sun/tanzania/arusha. Accessed: 2021-05-12.

[3] Duratherm 630. https://durathermfluids.com/products/duratherm-630/. Accessed: 2021-02-14.

[4] Electric power and energy. https://courses.lumenlearning.com/physics/chapter/20-4-electric-power-and-energy/. Accessed: 2021-2-3.

[5] Serial vs Parallel Connections Explained. https://www.renogy.com/learn-series-and-parallel/. Accessed: 2021-05-28.

[6] Solid mechanics. https://doc.comsol.com/5.5/doc/com.comsol.help.sme/sme_ug_solid.07.02.html. Accessed: 2021-05-14.

[7] K. E. Agbo, C. Walgraeve, J. I. Eze, P. E. Ugwoke, P. O. Ukoha, and H. Van Langenhove. A review on ambient and indoor air pollution status in africa. *Atmospheric Pollution Research*, 12(2):243–260, 2021.

[8] S.-C. Costa Pereira, K. Mahkamov, M. Kenisarin, M. Ismail, K. Lynn, E. Halimic, and D. Mullen. Solar salt latent heat thermal storage for a small solar organic rankine cycle plant. *Journal of Energy Resources Technology*, 142:1–11, 09 2019.

[9] C. W. Foong, O. J. Nydal, and J. Løvseth. Investigation of a small scale double-reflector solar concentrating system with high temperature heat storage. *Applied Thermal Engineering*, 31(10):1807–1815, 2011.

[10] Geiran M. S. Latent heat storage for frying, [project work]. *Department of Energy and Process Engineering. Norwegian University of Science and Technology – NTNU*, 2020.

[11] D. Jafari, A. Franco, S. Filippeschi, and P. Di Marco. Two-phase closed thermosyphons: A review of studies and solar applications. *Renewable and Sustainable Energy Reviews*, 53:575–593, 2016.

[12] S. Kalaiselvam and R. Parameshwaran. Chapter 5 - latent thermal energy storage. In S. Kalaiselvam and R. Parameshwaran, editors, *Thermal Energy Storage Technologies for Sustainability*, pages 83 – 126. Academic Press, Boston, 2014.

[13] S. Karekezi and W. Kithyoma. Renewable energy strategies for rural africa: is a pv-led renewable energy strategy the right approach for providing modern energy to the rural poor of sub-saharan africa? *Energy Policy*, 30(11):1071–1086, 2002. Africa: Improving Energy Services for the Poor.

[14] H. Mehling and L. F. Cabeza. *Solid-liquid phase change materials*, pages 11–55. Springer Berlin Heidelberg, Berlin, Heidelberg, 2008.

[15] S. Mondal. Phase change materials for smart textiles – an overview. *Applied Thermal Engineering*, 28(11):1536–1550, 2008.

[16] M. Mussard and O. Nydal. Comparison of oil and aluminum-based heat storage charged with a small-scale solar parabolic trough. *Applied Thermal Engineering*, 58:146–154, 09 2013.

[17] A. A. Parra and O. J. Nydal. Numerical and experimental investigation of two-phase thermosyphons coupled with latent and sensible thermal energy storages [unpublished manuscript]. *Department of Energy and Process Engineering. Norwegian University of Science and Technology – NTNU*, (2021).

[18] A. Saxena. 2013-solar cooking by using pcm as a thermal heat storage. 08 2013.

[19] J. Skovajsa, M. Koláček, and M. Zálešák. Phase change material based accumulation panels in combination with renewable energy sources and thermoelectric cooling. *Energies*, 10:152, 01 2017.

[20] K. Thaule S., Gustafson K. M. Dump loading to high temperature heat storage, [project work]. *Department of Energy and Process Engineering. Norwegian University of Science and Technology – NTNU*, (2018).

[21] S. Wu. 4 - heat energy storage and cooling in buildings. In M. R. Hall, editor, *Materials for Energy Efficiency and Thermal Comfort in Buildings*, Woodhead Publishing Series in Energy, pages 101 – 126. Woodhead Publishing, 2010.

A Duratherm 630 datasheet

DURATHERM
Heat Transfer Fluids

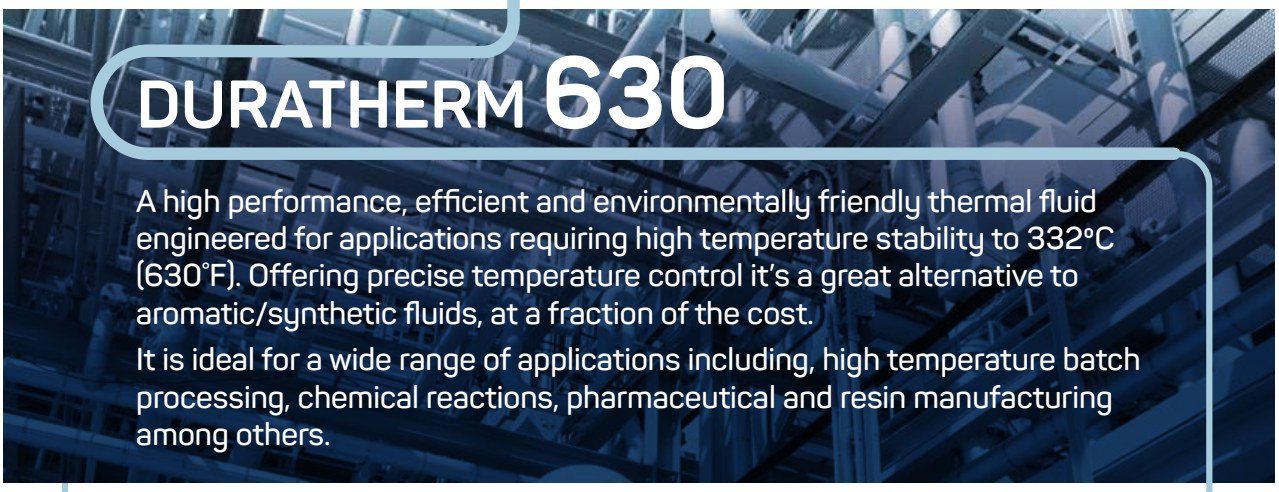

DURATHERM 630

A high performance, efficient and environmentally friendly thermal fluid engineered for applications requiring high temperature stability to 332°C (630°F). Offering precise temperature control it's a great alternative to aromatic/synthetic fluids, at a fraction of the cost.

It is ideal for a wide range of applications including, high temperature batch processing, chemical reactions, pharmaceutical and resin manufacturing among others.

APPLICATION

Duratherm 630 is a high performance, efficient and environmentally friendly fluid engineered for applications requiring high temperature stability to 332°C (630°F). Offering precise temperature control it's a great alternative to high temperature aromatic fluids, at a fraction of the cost.

It is ideal for a wide range of applications including, high temperature batch processing, chemical reactions, pharmaceutical and resin manufacturing among others.

THE DIFFERENCE

Our exclusive additive package, including a proprietary dual stage anti-oxidant, ensures long trouble free operation. **Duratherm 630** also incorporates metal deactivators, a seal and gasket extender, de-foaming and particle suspension agents.

LASTS LONGER

Oxidation can cripple your system. Left unchecked, it will ultimately cause catastrophic failure and costly downtime. That's why **Duratherm 630** offers unsurpassed levels of protection against oxidation, and a service life that other fluids simply can't match.

RUNS CLEANER

Duratherm 630 delivers superior resistance to sludging, a problem plaguing most other fluids. That makes it the best defense against extreme oxidation found in many of today's demanding manufacturing environments.

ENVIRONMENTAL

Duratherm 630 is environmentally friendly, non-toxic, non-hazardous and non-reportable. It poses no ill effect to worker safety and does not require special handling. After its long service life, **Duratherm 630** can easily be disposed of with other waste oils.

SYSTEM CLEANING

If your existing fluid has let you down and left you with a system full of sludge or carbon, we've developed a full line of heat transfer system cleaners to get your system back to like-new condition. Contact us for complete details.

1 800 446 4910

www.durathermfluids.com

1 of 4

DURATHERM 630

- Maximum temperature: 332°C / 630°F
- Flash point 229°C / 444°F
- Alternative to chemical aromatic fluids
- Non-toxic/non-hazardous
- Includes free fluid analysis and tech support

1 800 446 4910

www.durathermfluids.com

TEMPERATURE RATINGS

Maximum Bulk/Use Temp.	332°C	630°F
Maximum Film Temp.	354°C	670°F
Pour Point ASTM D97	-18°C	-1°F

SAFETY DATA

Flash Point ASTM D92	229°C	444°F
Fire Point ASTM D92	244°C	472°F
Autoignition ASTM E-659-78	368°C	693°F

THERMAL PROPERTIES

Thermal Expansion Coefficient	0.1011 %/°C	0.0562 %/°F
Thermal Conductivity	W/m K	BTU/hr F ft
38°C / 100°F	0.143	0.083
260°C / 500°F	0.131	0.076
316°C / 600°F	0.128	0.074
332°C / 630°F	0.127	0.073
Heat Capacity	kJ/kg K	BTU/lb F
38°C / 100°F	1.991	0.475
260°C / 500°F	2.724	0.650
316°C / 600°F	2.908	0.694
332°C / 630°F	2.962	0.707

PHYSICAL PROPERTIES

Appearance: colorless, clear and bright liquid		
Viscosity ASTM D445		
cSt at 40°C / 104°F	42.31	
cSt at 100°C / 212°F	6.82	
cSt at 316°C / 600°F	0.79	
cSt at 332°C / 630°F	0.74	
Density ASTM D1298	kg/m3	lb/ft3
38°C / 100°F	853.39	53.29
260°C / 500°F	702.45	43.85
316°C / 600°F	665.74	41.50
332°C / 630°F	652.5	40.79
Vapor Pressure ASTM D2879	kPa	psi
38°C / 100°F	0.00	0.00
260°C / 500°F	2.28	0.33
316°C / 600°F	9.75	1.40
332°C / 630°F	14.2	2.04
Distillation Range ASTM D2887	10%	383°C (721°F)
	90%	494°C (921°F)
Average Molecular Weight	395	

The values quoted are typical of normal production. They do not constitute a specification.

DURATHERM 630

PROPERTY VS. TEMPERATURE CHART
METRIC

TEMPERATURE (Celsius)	DENSITY (kg/m^3)	KINEMATIC VISCOSITY (Centistoke)	DYNAMIC VISCOSITY (Centipoise)	THERMAL CONDUCTIVITY (W/m-K)	HEAT CAPACITY (kJ/kg-K)	VAPOR PRESSURE (kPa)
-5	882.63	683.16	602.98	0.146	1.849	0.00
5	875.83	307.70	269.49	0.145	1.882	0.00
15	869.03	156.16	135.71	0.145	1.915	0.00
25	862.23	87.38	75.34	0.144	1.948	0.00
35	855.43	52.97	45.31	0.144	1.981	0.00
45	848.63	34.31	29.11	0.143	2.014	0.00
55	841.84	23.47	19.76	0.142	2.047	0.00
65	835.04	16.81	14.04	0.142	2.080	0.00
75	828.24	12.51	10.37	0.141	2.113	0.00
85	821.44	9.62	7.90	0.141	2.146	0.00
95	814.64	7.60	6.19	0.140	2.179	0.00
105	807.84	6.15	4.97	0.140	2.212	0.00
115	801.04	5.08	4.07	0.139	2.245	0.01
125	794.24	4.26	3.39	0.138	2.278	0.01
135	787.44	3.64	2.86	0.138	2.311	0.02
145	780.64	3.14	2.45	0.137	2.344	0.03
155	773.84	2.75	2.13	0.137	2.377	0.05
165	767.04	2.43	1.86	0.136	2.410	0.08
175	760.24	2.16	1.65	0.135	2.443	0.12
185	753.45	1.95	1.47	0.135	2.476	0.18
195	746.65	1.76	1.32	0.134	2.509	0.26
205	739.85	1.61	1.19	0.134	2.542	0.38
215	733.05	1.47	1.08	0.133	2.575	0.54
225	726.25	1.36	0.99	0.133	2.608	0.77
235	719.45	1.26	0.91	0.132	2.641	1.06
245	712.65	1.17	0.84	0.132	2.674	1.45
255	705.85	1.10	0.78	0.131	2.707	1.96
265	699.05	1.03	0.72	0.130	2.740	2.60
275	692.25	0.97	0.67	0.130	2.773	3.44
285	685.45	0.92	0.63	0.129	2.806	4.49
295	678.65	0.87	0.59	0.129	2.839	5.82
305	671.86	0.83	0.56	0.128	2.872	7.47
315	665.06	0.79	0.53	0.128	2.905	9.51
325	658.26	0.76	0.50	0.127	2.938	12.00
332	653.39	0.74	0.48	0.126	2.960	15.03

The values quoted are typical of normal production.
They do not constitute a specification.

DURATHERM 630

PROPERTY VS. TEMPERATURE CHART
STANDARD

TEMPERATURE (Fahrenheit)	DENSITY (lb/ft^3)	KINEMATIC VISCOSITY (Centistoke)	DYNAMIC VISCOSITY (Centipoise)	THERMAL CONDUCTIVITY (BTU/hr-F-ft)	HEAT CAPACITY (BTU/lb-F)	VAPOR PRESSURE (Psia)
15	55.29	1018.91	902.98	0.084	0.438	0.00
25	55.06	621.05	548.04	0.084	0.443	0.00
35	54.82	395.64	347.63	0.084	0.447	0.00
45	54.58	262.15	229.35	0.084	0.451	0.00
55	54.35	179.91	156.72	0.084	0.456	0.00
65	54.11	127.41	110.51	0.084	0.460	0.00
75	53.88	92.80	80.14	0.083	0.464	0.00
85	53.64	69.32	59.60	0.083	0.469	0.00
95	53.40	52.97	45.34	0.083	0.473	0.00
105	53.17	41.31	35.20	0.083	0.478	0.00
115	52.93	32.81	27.83	0.083	0.482	0.00
125	52.70	26.49	22.38	0.082	0.486	0.00
135	52.46	21.72	18.26	0.082	0.491	0.00
145	52.23	18.04	15.10	0.082	0.495	0.00
155	51.99	15.18	12.65	0.082	0.499	0.00
165	51.75	12.91	10.71	0.082	0.504	0.00
175	51.52	11.09	9.16	0.082	0.508	0.00
185	51.28	9.62	7.91	0.081	0.513	0.00
195	51.05	8.42	6.89	0.081	0.517	0.00
205	50.81	7.42	6.04	0.081	0.521	0.00
215	50.57	6.59	5.34	0.081	0.526	0.00
225	50.34	5.88	4.75	0.081	0.530	0.00
235	50.10	5.29	4.25	0.080	0.534	0.00
245	49.87	4.78	3.82	0.080	0.539	0.00
255	49.63	4.34	3.46	0.080	0.543	0.00
265	49.40	3.97	3.14	0.080	0.548	0.00
275	49.16	3.64	2.87	0.080	0.552	0.00
285	48.92	3.35	2.63	0.080	0.556	0.00
295	48.69	3.09	2.42	0.079	0.561	0.01
305	48.45	2.87	2.23	0.079	0.565	0.01
315	48.22	2.67	2.06	0.079	0.569	0.01
325	47.98	2.49	1.92	0.079	0.574	0.01
335	47.75	2.33	1.79	0.079	0.578	0.02
345	47.51	2.19	1.67	0.079	0.583	0.02
355	47.27	2.06	1.56	0.078	0.587	0.02
365	47.04	1.95	1.47	0.078	0.591	0.03
375	46.80	1.84	1.38	0.078	0.596	0.03
385	46.57	1.74	1.30	0.078	0.600	0.04
395	46.33	1.66	1.23	0.078	0.604	0.05
405	46.09	1.58	1.16	0.077	0.609	0.06
415	45.86	1.50	1.10	0.077	0.613	0.08
425	45.62	1.43	1.05	0.077	0.618	0.08
435	45.39	1.37	1.00	0.077	0.622	0.11
445	45.15	1.31	0.95	0.077	0.626	0.13
455	44.92	1.26	0.91	0.077	0.631	0.15
465	44.68	1.21	0.87	0.076	0.635	0.19
475	44.44	1.17	0.83	0.076	0.639	0.22
485	44.21	1.12	0.80	0.076	0.644	0.26
495	43.97	1.08	0.76	0.076	0.648	0.31
505	43.74	1.05	0.73	0.076	0.653	0.36
515	43.50	1.01	0.71	0.076	0.657	0.42
525	43.26	0.98	0.68	0.075	0.661	0.48
535	43.03	0.95	0.65	0.075	0.666	0.56
545	42.79	0.92	0.63	0.075	0.670	0.66
555	42.56	0.89	0.61	0.075	0.674	0.76
565	42.32	0.87	0.59	0.075	0.679	0.87
575	42.09	0.84	0.57	0.074	0.683	1.00
585	41.85	0.82	0.55	0.074	0.688	1.14
595	41.61	0.80	0.53	0.074	0.692	1.31
605	41.38	0.78	0.52	0.074	0.696	1.49
615	41.14	0.76	0.50	0.074	0.701	1.69
625	40.91	0.74	0.49	0.074	0.705	1.92
630	40.79	0.74	0.48	0.073	0.707	2.04

The values quoted are typical of normal production.
They do not constitute a specification.

B Fyrewrap datasheet

When Fire Protection Matters Most
Contact your local distributor.

Unifrax Ltd.
T:+44 (0)1744 88 7600 F: +44 (0)1744 88 9916
www.unifrax.com

DESCRIPTION

FyreWrap® LT Blanket from Unifrax is a new lightweight, & flexible high temperature insulation blanket manufactured from Insulfrax low bio-persistence fibres & is specifically designed for passive fire protection applications.

With its enhanced fibre properties, FyreWrap LT Blanket offers significant weight savings when compared with both traditional AES wool blankets and more particularly mineral wool based products. The modified fibre characteristics also give FyreWrap LT Blankets improved handling characteristics.

Thin, lightweight systems, combined with a flexible and easy to install form result in lower installation costs and significant weight savings. The fibres are totally inorganic and FyreWrap LT Blanket contains no binder no smoke or fumes are generated when exposed heat.

FIRE PROTECTION PROPERTIES

- Non Combustible to IMO FTP Code Part 1
- Classified A1 to EN 13501-1

BV 2690

TYPICAL APPLICATIONS

Unifrax FyreWrap LT Blanket is suitable for use in a wide variety of passive fire protection applications including:

- Marine deck and bulkhead insulation in all types of craft
- Hydrocarbon and jet fire protection of vessels and pipes
- Bulkhead & deck insulation for offshore oil platforms & FPSO's
- Cable tray fire protection
- Ductwork fire protection
- Infill of fire doors and lightweight cladding panels

Any new and/or special use of these products, whether or not in an application listed in our literature, must be submitted to our technical department for their prior written approval.

FyreWrap® LT Blanket

TYPICAL PRODUCT PARAMETERS

Thermal Characteristics

Ambient Insulation Performance

Blanket Thickness (mm)	R Value	U Value
25	0.78	1.28
40	1.25	0.80
45	1.41	0.71
50	1.56	0.64
55	1.72	0.58

Based on thermal conductivity of FyreWrap LT Blanket 64 kg/m³ density measured to BS EN 12667 at 10°C of 0.0320 W/mK. For blanket densities above 64kg/m³ the same values may be used.

Thermal Conductivity (W/mK)

Mean Temp. (°C)	64kg/m³	96kg/m³	128kg/m³
200	0.06	0.06	0.05
400	0.11	0.09	0.08
600	0.17	0.14	0.12
800	0.26	0.20	0.18
1000	0.38	0.29	0.25

Thermal Conductivity measured in accordance with ASTM C-201.

Acoustic Characteristics

Sound Absorption

Frequency (Hz)	50mm x 70kg/m³	50mm x 96kg/m³
125	0.47	0.26
250	1.05	0.94
500	1.09	1.03
1000	1.09	1.03
2000	1.12	1.09
4000	1.12	1.14
5000	1.18	1.09
NRC	**1.10**	**1.00**

Test method BS EN ISO 354:2003. Foil facing will reduce the sound absorption characteristics.

Blanket Facings

FyreWrap LT Blanket can be supplied faced with choice of facing. The following grades are available :

FyreWrap LTF Blanket with 30µm foil on one face.

FyreWrap LTFR Blanket with 30µm foil & glass fibre mesh reinforcement on one face.

FyreWrap LTG Blanket with glass fibre cloth on one face.

FyreWrap LTFE Blanket is fully encapsulated in a 200µm reinforced aluminium composite scrim.

FyreWrap LTF, LTFR & LTG blankets are available with the covering on both top and bottom surfaces of the blanket and are designated LTF2, LTFR2, and LTG2 respectively.

AVAILABILITY

Standard Roll Sizes

Thickness (mm)	Roll Length (m)	Density (kg/m³)
25	7.32	64,96,128
35	5.0	70
38	5.0	96, 128
40	5.0	70
45	5.0	64
50	3.66	64, 70, 96,128
55	3.66	64, 70

Standard roll width is 610mm or 1220mm. Other sizes may be available on request subject to minimum order requirements. FyreWrap LT Blanket may also available as WR grade in which the fibres are lightly coated with a water repellent silicone treatment.

HANDLING INFORMATION

A Material Safety Data Sheet has been issued describing the health, safety and environmental properties of this product, identifying the potential hazards and giving advice on handling precautions and emergency procedures. This must be consulted and fully understood before handling, storage or use.

Supplied by:

C PV Controller

MPPT Load Controller

Documentation
Rev. 2
Feb 2020 - Odin Hoff Gardå

Features

- 6 thermocouple inputs
- DC/DC buck converter
- P&O MPPT
- Proportional voltage MPPT
- RMS power measurement
- Datalogging to microSD card and real-time clock.
- Manual load adjustment mode

Maximum ratings

Parameter	Min	Nominal	Max	Unit
Voltage (single panel)	16	38	40	V
Voltage (6 panels in series)	96	220	230	V
Load current	0		10	A
Aux. power voltage	16	24	42	V

WARNING: Parts at high voltage potential are exposed inside the enclosure. Connection should only be done by a qualified person.

WARNING: Always make sure polarity and voltages are correct. Reverse polarity and over-voltage can destroy the system.

1

Quick start guide

Content: PC with remote monitoring software, PC power supply, Load controller, box with accessories: USB cable, microSD card adapter, spare Wago connectors.

How to connect PV panels and load (heater):

Connect PV panels and load using the pre-attached Wago lever-connectors.

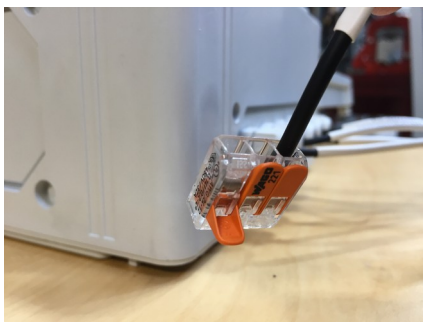

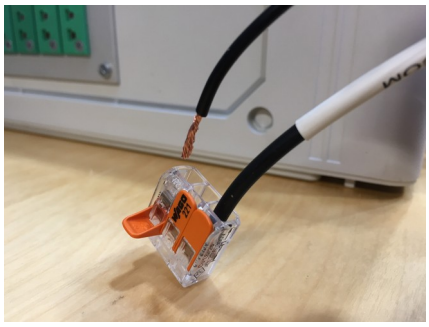

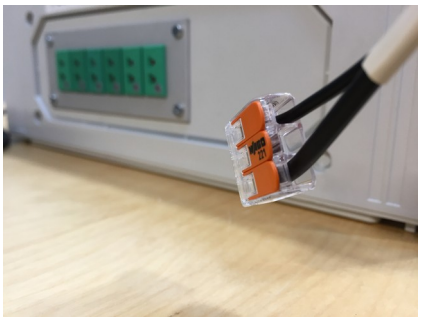

1. Pull lever down.
2. Insert stripped wire (Use maximum 4 mm2 copper wire.)
3. Press lever all the way back to lock the wire in place.
4. Please make sure connection is good both electrically and mechanically by visual inspection and pulling the wire respectively.

Connections (Follow the steps in the correct order. See connection diagram below as well.)

1. Turn main switch to OFF position.
2. Connect LOAD (Heater) to the wires marked LOAD HEATER + and LOAD HEATER -. The polarity of the load does not matter.
3. Connect the 0V (Minus/Negative) of the lowest panel in the PV array to the wire marked PV ARRAY: 0V/COM.
4. Connect the plus/positive from the top panel in the PV array to the wire marked PV ARRAY: +220V DC. **(WARNING: High voltage)**
5. Connect the plus/positive from the **lowest (!)** panel in the PV array to the wire marked PV ARRAY: +38V DC.
6. **Before** turning the main switch to the ON-position, carry out the measurements descibed on the next page. **(Reverse polarity or over-voltage can completely destroy the controller)**
7. If all measurements are good, turn the main switch ON.

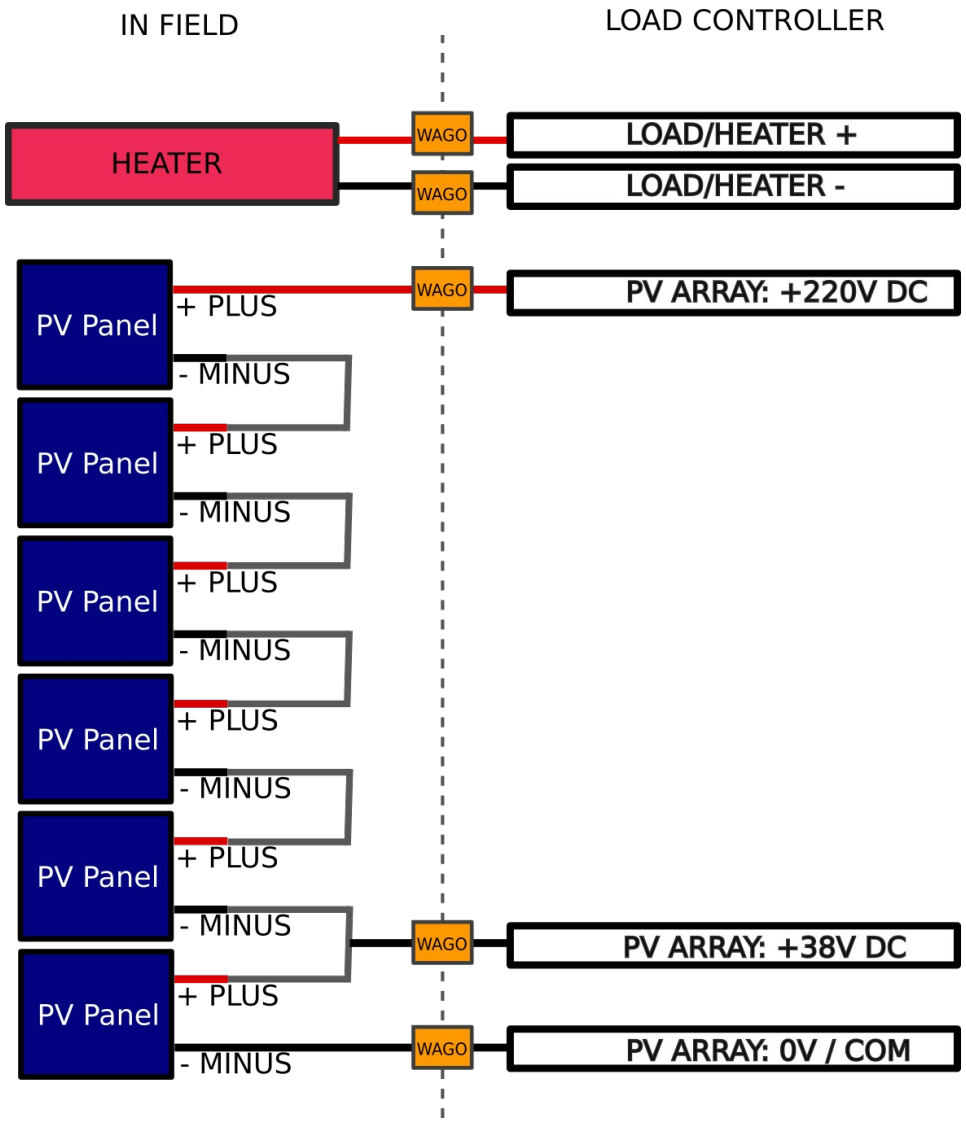

Pre-startup tests (please do not skip these)

Connect the **red** test lead to the **V** input of your multimeter and the **black** test lead to the **COM** input.

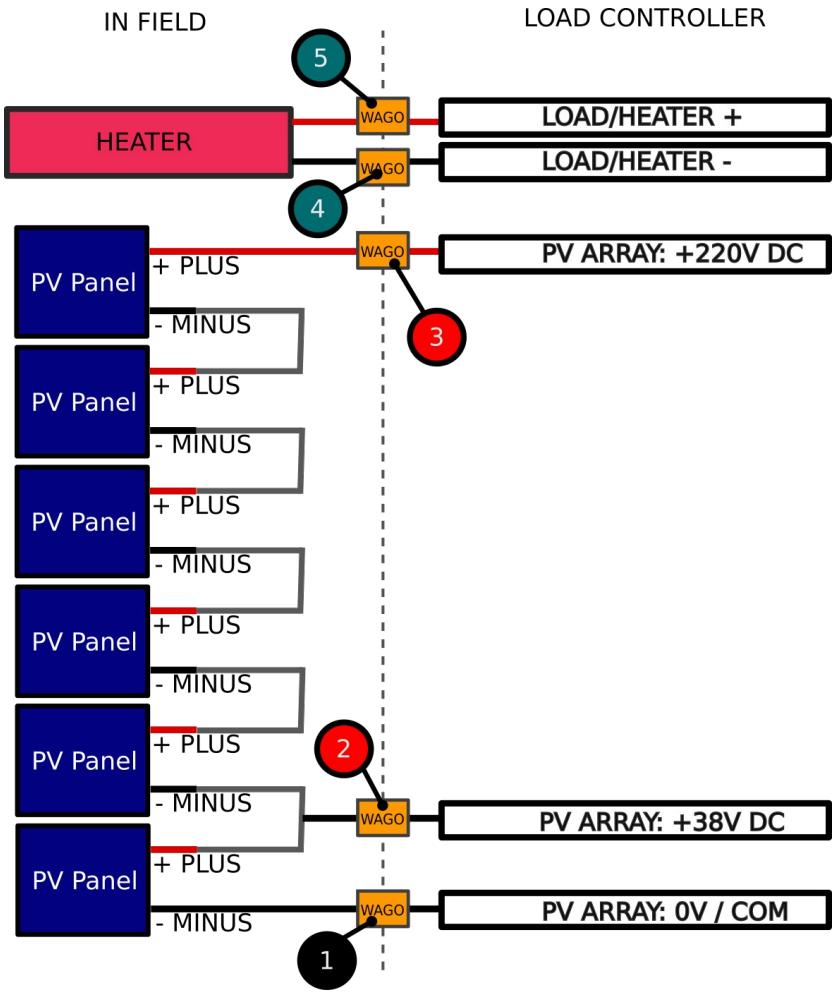

Use a multimeter that can measure DC voltage and resistance. Put the test leads in the Wago connectors.

1. Put the multimeter into resistance mode and measure the resistance between **4** and **5**.
   It should be in the range 10-50Ω (Ohms).
2. Put the multimeter into DC voltage mode and connect the black lead (COM) to **1**.
3. Use the red lead (V) to measure the voltage at **2**.
   *It should be in the range 30-39V DC. The voltage should **not** be negative.*
4. Now take the red lead (V) and measure the voltage at **3**.
   *It should be in the range 180-234V DC. The voltage should **not** be negative.*

If all measurements are within range, the system can be switched ON.

Connect thermocouples with type K miniature plug on the side of the box (The connectors only fit one way around.):

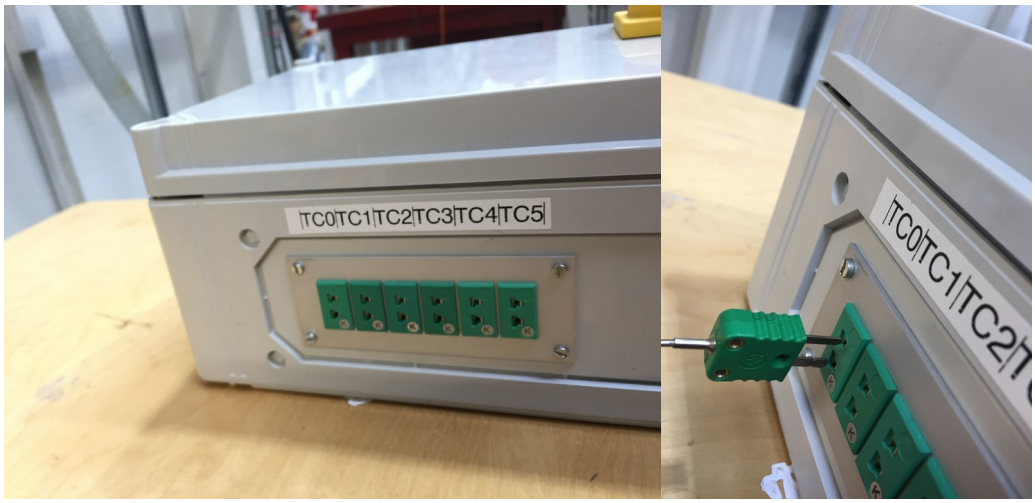

Note: Please place the controller box in a shaded area if possible to keep the temperatures as low as possible.

Overview:

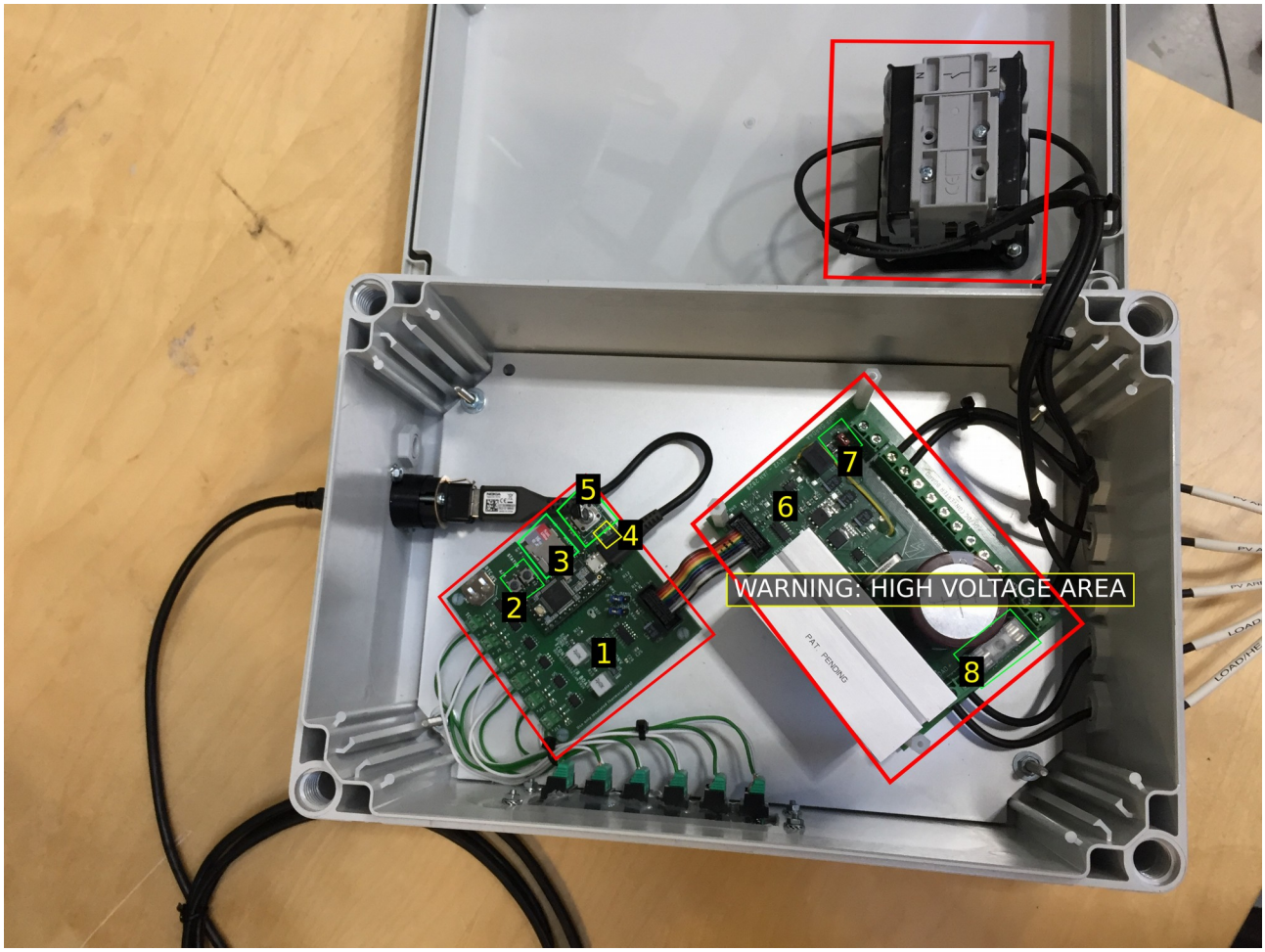

1. Low voltage controller board 2. Push buttons S1 and S2 3. microSD card

4. Status LEDs 5. Potmeter for manual PWM control 6. High voltage power board

7. AUX power jumper 8. Main fuse

How to use the PC monitor software

1. Connect USB cable to the load controller and PC.


2. Make sure the controller is powered on.
3. Double-click the LoadController software shortcut on the desktop.

4. Choose COM port (usually COM4) and press «NEXT >>»

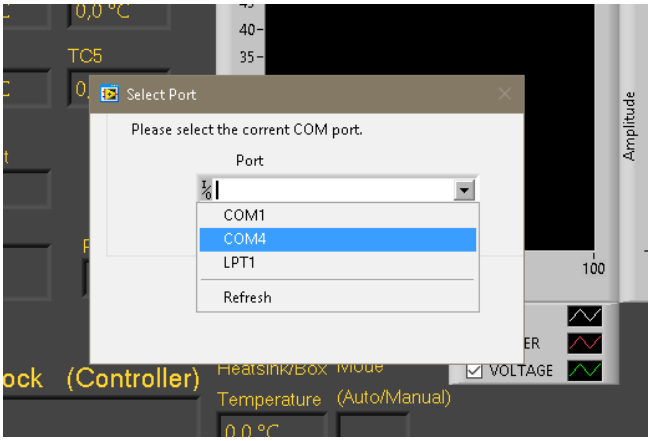

You should now be able to read real-time measurements including: thermocouples, voltage, current, power and PWM output to the DC/DC converter. If nothing happens, try turing the power off and on again on the controller box and restart the software on the PC.

Note: If the Heatsink temperature gets above 40-50 degrees C, consider opening the controller box to reduce the temperature.

Note: Data is logged to files on the computer (in the folder LogFiles on desktop).

How to extract logged data from SD card:

1. Turn power off completely.
2. Disconnect the USB cable to access the SD card.
3. Push the SD card into the socket and release.
4. Put the SD card into the microSD-to-SD adapter.
5. Put the SD card into an appropriate card reader and copy the file «log.txt».
6. (Delete the file «log.txt» on the SD card to clear logged data from the controller.)
7. Push the SD card back into the socket on the controller board.
8. Reconnect the USB cable
9. Import as tab-separated CSV into Excel or similar software.

LEDs and push buttons functionality

S1 (A/M): Toggles between auto and manual control. In auto mode, a MPPT algorithm is controlling the load. In manual mode, the PWM duty cycle is controlled using the on-board potentiometer.

Thermocouples

There are six thermocouple inputs. The temperature measurements are logged to SD card. The circuit uses six MAX31855 thermocouple amplifier and communicate with the microcontroller using SPI.

Troubleshooting for thermocouples:

Check the following points:

1. Polarity and connections are correct. (+ and - are marked on the PCB next to screw terminals.)
2. Thermocouple is of type K.
3. Thermocouple is of insulated type (e.g. mineral insulated).
4. Thermocouple and/or wire is not broken.

Certain errors can be detected by the controller board. In that case, the temperature reads as follows:

Temperature reading	**Error**	**Fix**
-1000.0	Open circuit	Check thermocouple and connections.
-2000.0	Short to VCC or GND	Check thermocouple. Make sure the thermocouple is insulated. (Electrically disconnected from sleeve)
-3000.0	Other	If the list above does not fix it, something is probably broken.

microSD card

Use only a microSD card formatted to a FAT32 or FAT16 file system. To do this on Windows, use an microSD to SD adapter if needed, right-click the SD card volume in «My Computer» and click format. Choose FAT32 or FAT16 filesystem and perform the formatting.

The log file is named «LOG.TXT».

To clear the logged data, delete the log file. The controller will automatically create a new one.

The data is tab separated and can be imported into your favourite spreadsheet software. The data is always on the following form:

Time	**TC0** (°C)	**TC1** (°C)	**TC2** (°C)	**TC3** (°C)	**TC4** (°C)	**TC5** (°C)	**Voltage** (V)	**Current** (A)	**Power** (W)	**Thermistor** (°C)	**PWM out** (%)

Replacing the fuse

WARNING: Always completely disconnect power before replacing the fuse!

Use 8 or 10A, 5x20mm fuse with voltage rating at least 250VDC.

Instructions for replacing fuse:

1. Disconnect power completely! Check using multimeter.
2. Remove fuse cover.
3. Remove old fuse and replace with new suitable fuse.
4. Attach fuse cover.
5. Reconnect power.

If the fuse trips: Check that the load is not shorted by measuring its resistance. Check connections, terminals and wires for damage.

Simplified system diagram

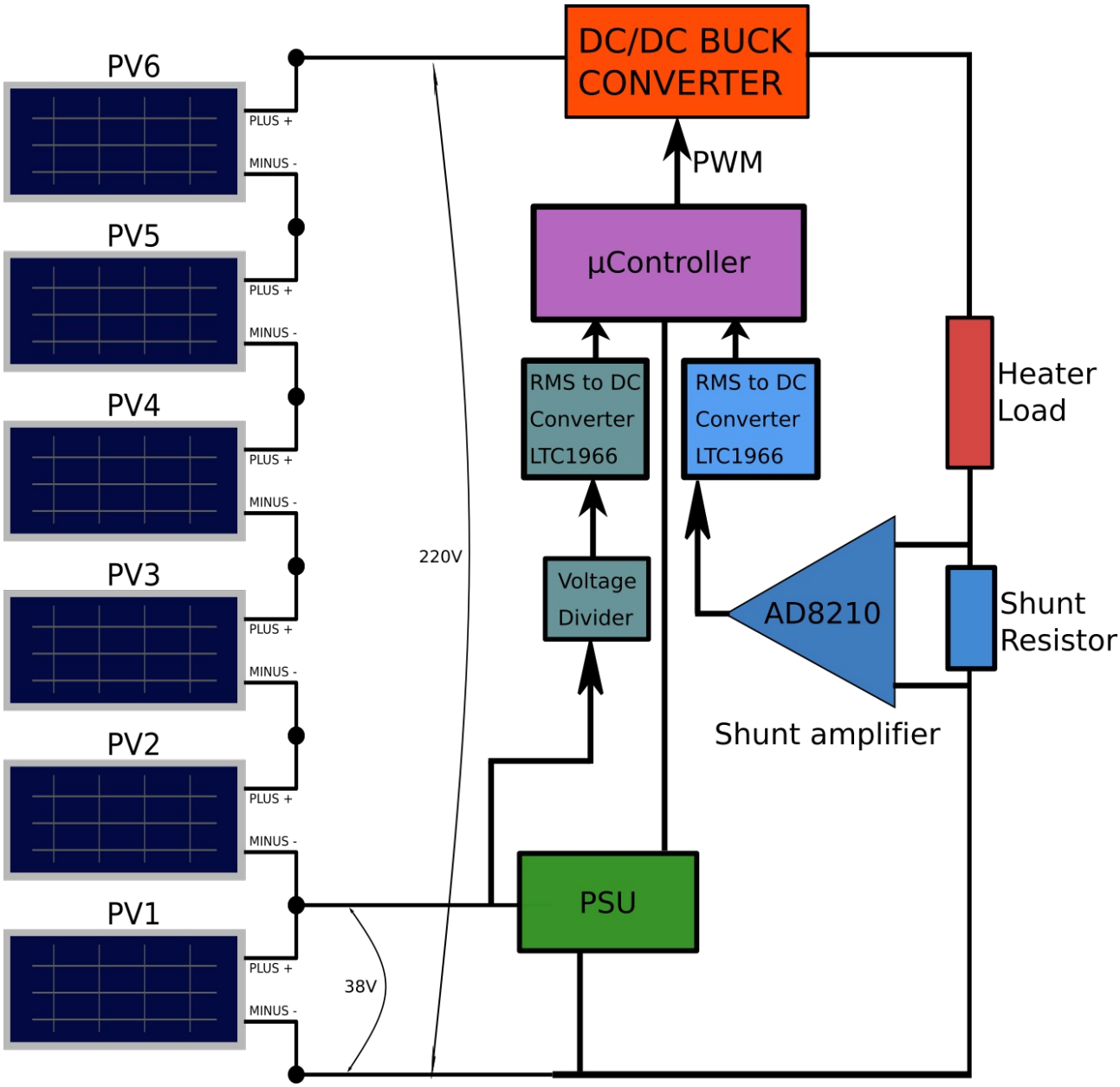

Auxiliary power connection

External power can be connected to drive the controller board so that datalogging and temperatures are logged even when there is no power from the solar PV array present. The voltage must be between 16V and 42V DC. **Do not reverse the polarity.**

AUX power jumper near the connection terminals must be set from **PV** to **AUX**.

RMS voltage and current measurements

The voltage of the lowest panel (PV1) is measured and multiplied by the number of panels to approximate the total voltage of the PV array. RMS calculations are done in hardware using LTC1966 RMS to DC converters.

The current is measured using a 0.025 Ohm shunt resistor together with a current shunt amplifier (AD8210). As with voltage, the RMS is computed using either software or with LTC1966.

Maximum Power Point Tracking (MPPT)

The algorithm begins by the following **pre-tracking routine**:

1. Measure the open circuit voltage.
2. Increase the load until voltage has decreased 10% from the open circuit voltage.
3. Pre-Tracking complete, start MPPT

The MPPT algorithm is of the standard «perturb and observe» type (P&O).

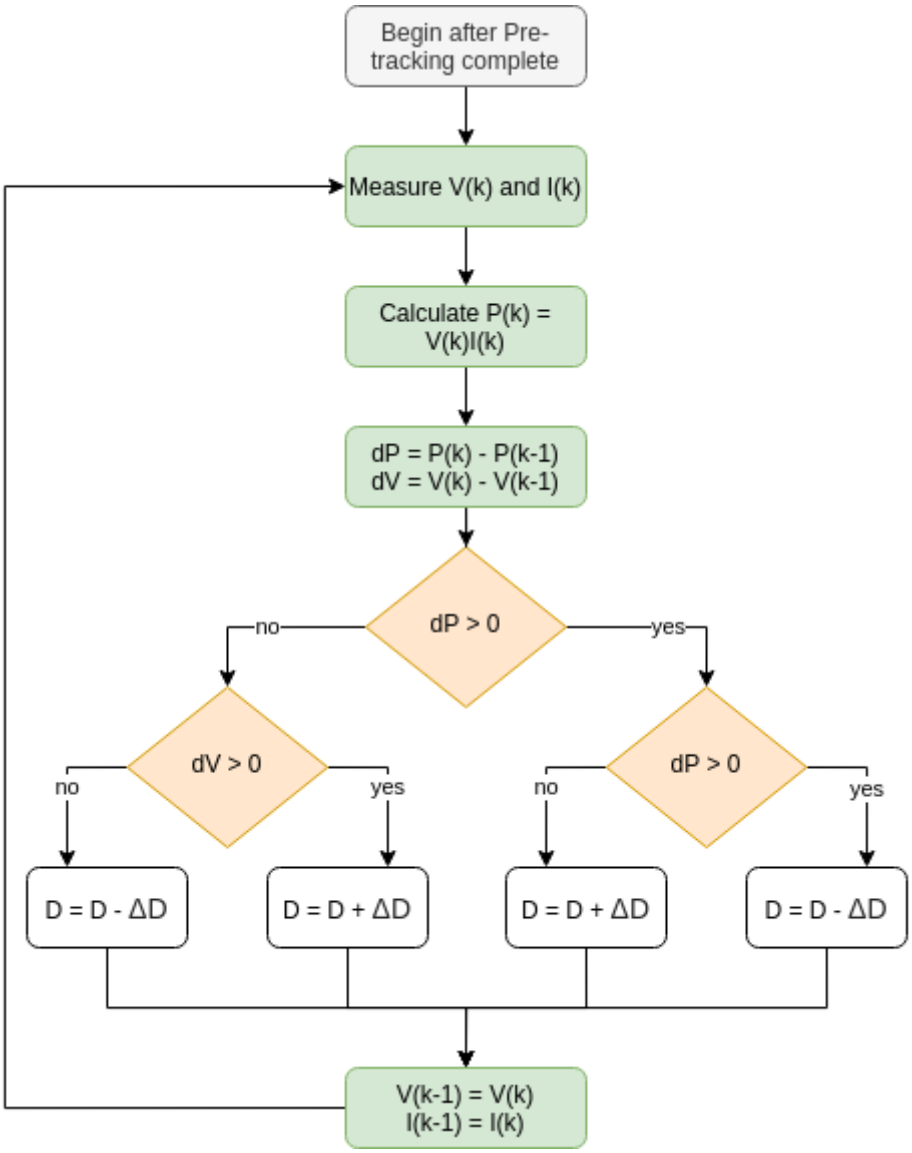

V(k) Voltage at time k
I(k) Current at time k
D PWM Duty cycle
ΔD Stepsize

Note: In the actual implementation, the stepsize depends on the system voltage.

I/O overview for programming (Teensy 3.2)

MAX31855 SPI

Pin function	Pin	Description/Notes
TC0 CS	14	Chip select (active low w/ external pullup)
TC1 CS	15	Chip select (active low w/ external pullup)
TC2 CS	16	Chip select (active low w/ external pullup)
TC3 CS	17	Chip select (active low w/ external pullup)
TC4 CS	18	Chip select (active low w/ external pullup)
TC5 CS	19	Chip select (active low w/ external pullup)
HW SPI SCK	13	HW SPI clock line
HW SPI DI (MISO)	12	HW SPI Master In Slave Out
SW SPI SCK	20	SW SPI clock line
SW SPI DI (MISO)	10	SW SPI Master In Slave Out

Note: Jumper JP1 and JP4 on controller board PCB must be changed if SW/bit banged SPI is to be used.

microSD SPI

Pin function	Pin	Description/Notes
HW SPI SCK	13	HW SPI clock line
HW SPI DI (MISO)	12	HW SPI Master In Slave Out
microSD CS	2	Chip select (active low w/ external pullup)
HW SPI DO (MOSI)	11	HW SPI Master Out Slave In
microSD CD	3	Card detect switch (low = card inserted)

Analog inputs

Pin function	Pin	Description/Notes
TEMP	A7/21	NTC thermistor for thermal shutdown
VSENSE	A8/22	RAW or RMS voltage
ISENSE	A9/23	RAW or RMS current
POT	A10	Potentiometer for manual PWM control

Note: Jumpers JP2 and JP3 can be used to change between RAW or RMS input. RAW input requires software RMS calculations, RMS input uses the LTC1966 DC to RMS converter.

Digital inputs

Pin function	Pin	Description/Notes
S1	6	Push button S1 Auto/Manual (active high w/ external pulldown)
S2	4	Push button S2 Status (active high w/ external pulldown)

Digital outputs

Pin function	Pin	Description/Notes
PWM	5	PWM output to MOSFET driver chip (external pulldown)
D1	9	Status LED D1
D2	8	Status LED D2
D3	7	Status LED D3

Special assembly instructions (rev2)

Assembly notes Teensy 3.2:

- Cut trace to Vin from USB power
- Solder on RTC crystal on Teensy
- Connect reset signal to reset pad

Mount NTC thermistor on heatsink by M3 screw.
Solder thin wire from reset pad on Teensy 3.2 to the reset pad on the controller board.
Hot glue capacitor and heatsink for support.

D USB TC-08 8 Channel Thermocouple Data Logger

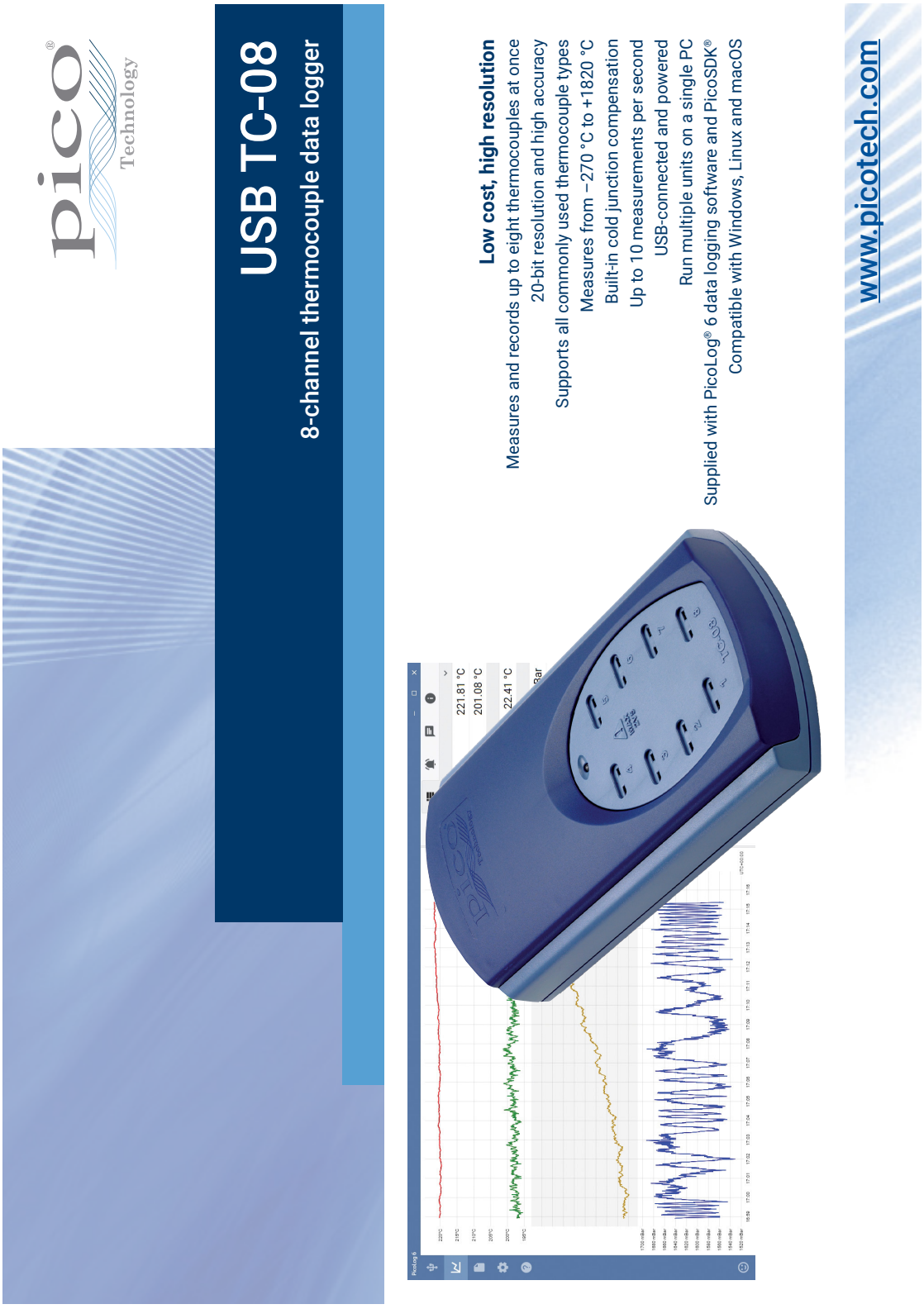

USB TC-08 thermocouple data logger

The USB TC-08 thermocouple data logger offers industry-leading performance and a cost-effective temperature measurement solution. With eight direct thermocouple inputs, the USB TC-08 can take accurate, rapid readings. In addition, you can use up to 20 units simultaneously on one PC. The logger can measure and record temperatures ranging from –270 °C to +1820 °C using the appropriate thermocouple type (B, E, J, K, N, R, S, T). It draws power from your computer's USB port, so no external power supply is necessary.

Wide temperature range

The USB TC-08 thermocouple data logger is designed to measure a wide range of temperatures using any thermocouple that has a miniature thermocouple connector. Pico supplies a wide range of suitable thermocouples (see **Ordering information**).

All types of thermocouple in common use today are supported, allowing an effective temperature range of –270 °C to +1820 °C (the actual temperature range depends on the thermocouple being used).

You can also use the built-in cold junction compensation (CJC) circuit as a ninth channel to measure ambient temperature.

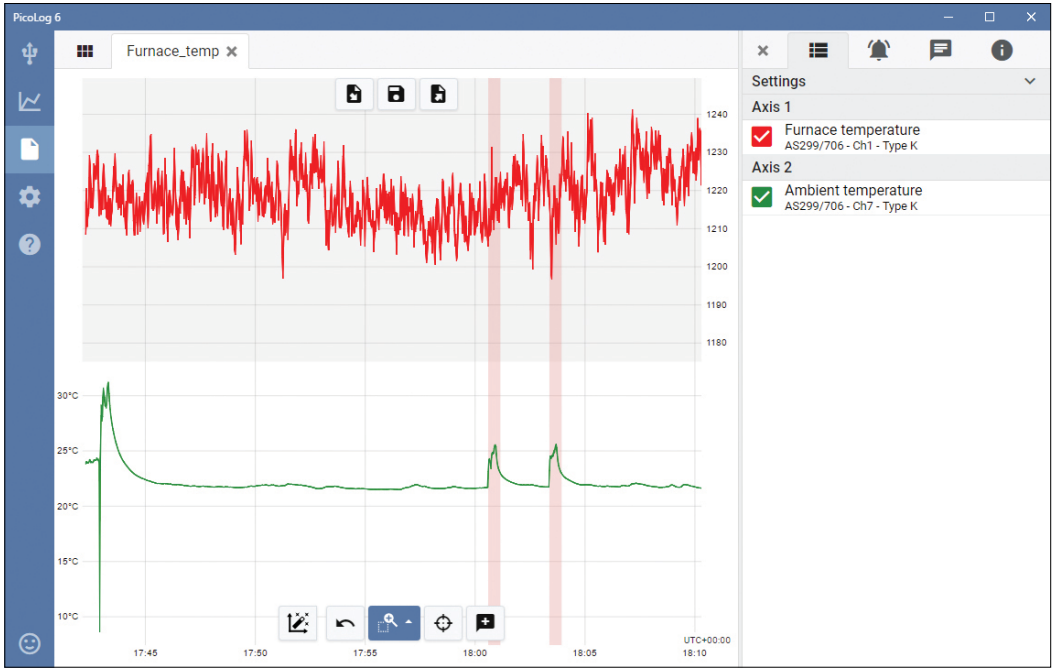

Fast and accurate temperature data acquisition

With the USB TC-08 thermocouple data logger, you can make temperature measurements both quickly and accurately.

The short conversion time of the USB TC-08 means that it can take up to 10 temperature measurements every second (CJC counts as an additional measurement), while the high (20-bit) resolution ensures that the USB TC-08 can detect minute changes in temperature. For Type K thermocouples, the USB TC-08 can maintain a better than 0.025 °C resolution over a –250 °C to +1370 °C range.

PicoLog 6 software – straightforward from the start

PicoLog 6 is a complete data acquisition software package for the TC-08 data logger, and is fully compatible with Windows, macOS and Linux. With its clear and user-friendly layout, ideal for use with a mouse or a touchscreen, PicoLog 6 allows you to set up the logger and start recording with just a few clicks of the mouse, whatever your level of data logging experience. Set up simple or advanced acquisitions quickly, and record, view and analyze your data with ease.

Capture controls
Separate **Record**, **Pause** and **Reset** buttons make it harder to press any of them by mistake.

Save and Export options
Copy your graph to the clipboard, save it as a PDF, export the raw data to a CSV file, or save the data and configuration as a robust `.picolog` database file.

Alarms
Set up alarms to alert you to a range of events. Alarms can take the form of sounds, visual notifications, graph annotations and more.

Notes & annotations
Add notes about the dataset as a whole or annotations about particular points on the graph.

Device settings view
Easily set up and adjust acquisition and math channels on one or more data loggers and check their status at a glance.

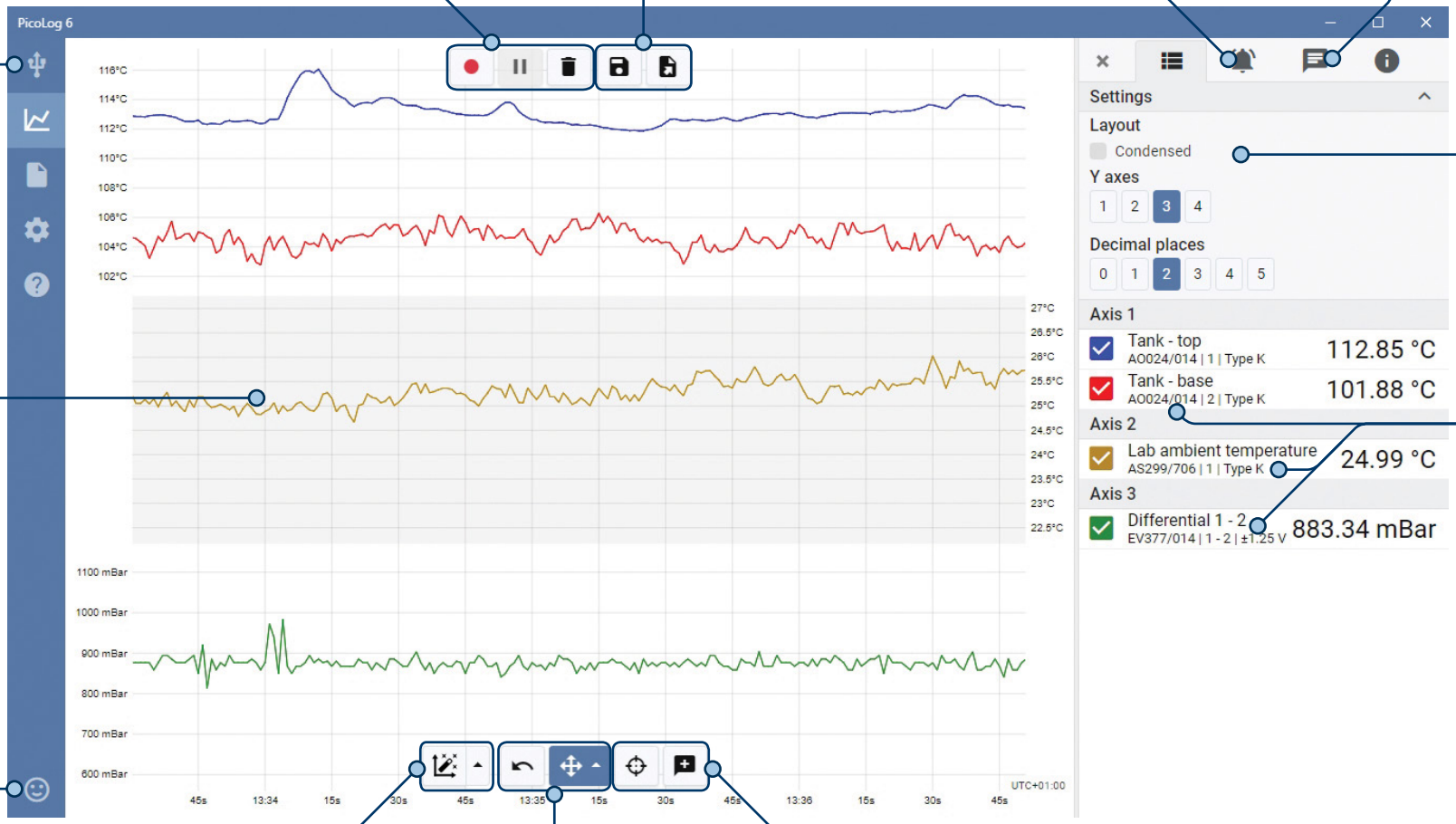

Pullout information panel
Manage your channel and axis settings, alarms, notes and capture information in this easy-to-read layout. Close the panel to make more room for the capture graph, and reopen it at any time.

Graph view
Display your data in real time, as it is collected, on up to four independent Y axes simultaneously: set them up by dragging and dropping the entries in the **Channels & Axes** panel on the right.

Multiple devices
Log data on up to 20 devices at the same time. Here, three separate data loggers are in use: two USB TC-08s and one ADC-24 voltage input logger.

Give instant feedback
We want to hear from you! Click here to contact Pico with your comments.

Data view
Display all the data collected so far or keep the graph scale the same and pan along as new samples appear.

Pan and zoom controls
Zoom in, zoom out, zoom to a selection or pan through the data with these tools. If you make a mistake, just click **Undo**.

Cursors and annotations
Use cursors to highlight the data value and time at any point on the graph, or click **Add annotation** to mark that point with a text note.

Math channels

Sometimes you need to use data from one or more measurement channels to graph and record a calculated parameter. You can use the PicoLog 6 equation editor to set up simple math channels such as A–B or more complex functions such as log, sqrt, abs, round, min, max, mean and median.

PicoLog 6 treats math channels like any other channel, so you can still set alarms and annotate them.

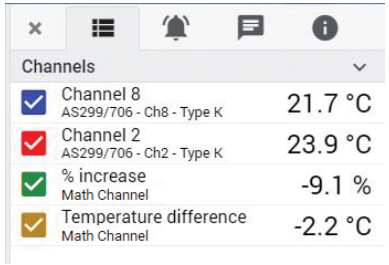

Alarms

In PicoLog 6, you can set up alarms to alert you to various events. These can be as simple or as complex as you like: alarms can trigger on a signal threshold or disconnection of the data logger, or you can set up a logic expression of your own. Alarms can play sounds, display visual alerts, run applications or mark when the event occurred on the graph.

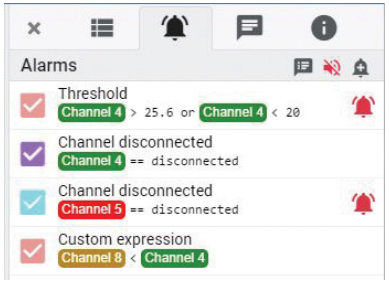

Intuitive logger and channel setup

The **Devices** view lets you set up a multichannel acquisition system in a simple way, with the option to use multiple different Pico data loggers simultaneously. PicoLog shows you an image of each connected device, so you can quickly and easily enable or disable channels and set up their properties.

On the right, you can see the device setup for the acquisition on the previous page: two USB TC-08s and one ADC-20 voltage input logger.

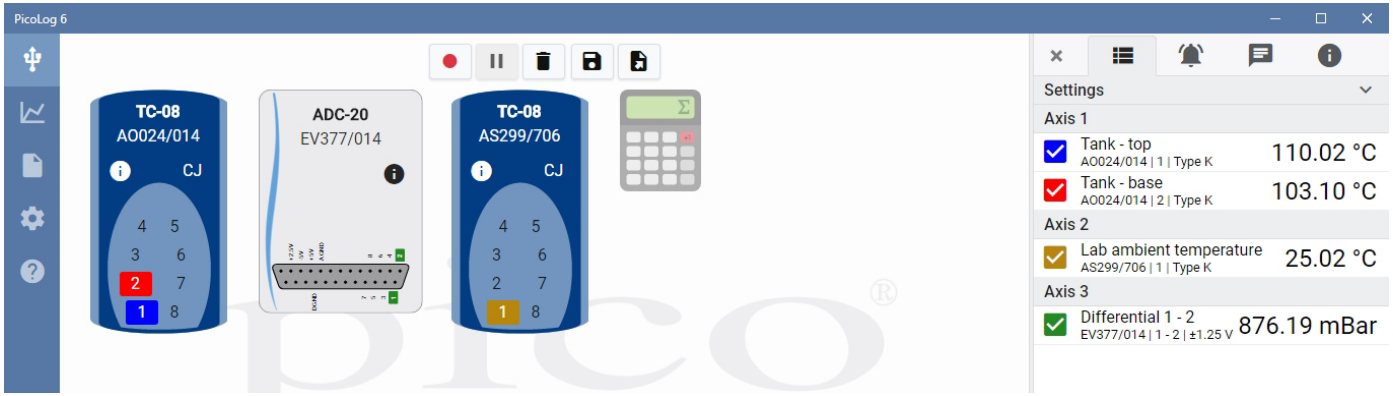

Robust file format

At the heart of PicoLog 6 is the file system, which stores live capture data directly to a robust database, rather than to a single file that is vulnerable to corruption and data loss. If the computer is shut down and rebooted, PicoLog will only lose the data during the outage – saving resumes when you restart the software.

This file system also means that the size of the dataset you can capture you is virtually unlimited – the only restriction is the size of your computer's hard disk!

The `.picolog` file format is compatible across all operating systems, and there is no need to set up a file to save to before the capture is complete. You can also save mid-capture if you wish to share the data collected so far. Since anyone can download and install PicoLog 6 for free, you can easily share saved data with co-workers, customers and suppliers for offline post-analysis.

PicoSDK®

Pico's software development kit, PicoSDK, is available free of charge and allows you to write your own software and interface to third-party software packages.

Pico also maintains repositories of example code on GitHub (github.com/picotech), showing how to use PicoSDK with software packages such as Microsoft Excel, National Instruments LabVIEW and MathWorks MATLAB, or with programming languages including C, C++, C# and Visual Basic .NET.

PicoSDK and the *USB TC-08 Programmer's Guide* are available to download from www.picotech.com/downloads.

Try the PicoLog 6 software today!

PicoLog 6's built-in demo mode allows you to try out the full functionality of the software with a choice of virtual devices and simulated live data. You also can use PicoLog 6 to view previously saved data, even with no device connected. Visit www.picotech.com/downloads and select **PicoLog Data Loggers** to get your copy.

Specifications

Hardware	
Number of channels (single unit)	8
Maximum number of channels (using up to 20 units)	160
Conversion time	100 ms per thermocouple channel + 100 ms for CJC (this can be disabled if all channels are used as voltage inputs)
Temperature accuracy	Sum of ±0.2% of reading and ±0.5 °C
Voltage accuracy	Sum of ±0.2% of reading and ±10 µV
Overvoltage protection	±30 V
Maximum common-mode voltage	±7.5 V
Input impedance	2 MΩ
Input range (voltage)	±70 mV
Resolution	20 bits
Noise-free resolution	16.25 bits
Thermocouple types supported	B, E, J, K, N, R, S, T
Input connectors	Miniature thermocouple

General	
Connectivity	USB 2.0
Device connector type	USB 2.0, Type B
Power requirements	USB port
Dimensions	201 x 104 x 34 mm (7.91 x 4.09 x 1.34 in)
Temperature range, operating	0 °C to 50 °C
Temperature range, operating, for quoted accuracy	20 °C to 30 °C
Temperature range, storage	−20 °C to 60 °C
Humidity range, operating	5 to 80 % RH non-condensing
Humidity range, storage	5 to 95 % RH non-condensing
Altitude	Up to 2000 m
Pollution degree	Pollution degree 2
Water resistance	Not water-resistant
Safety approvals	Designed to 2014/35/EU: Low Voltage Directive
EMC approvals	Tested to 2014/30/EU: Electromagnetic Compatibility Directive
Environmental approvals	RoHS and WEEE compliant
Software	PicoLog 6, PicoSDK (available from www.picotech.com/downloads) Example code (available from Pico's GitHub organization page, github.com/picotech)

General (continued)	
PC requirements	Windows 7, 8 or 10, 32-bit or 64-bit macOS 10.9 (Mavericks) or later, 64-bit only Linux (tested on Redhat, OpenSUSE and Ubuntu), 64-bit only Hardware as required by the operating system
Documentation	Quick Start Guide User's Guide Programmer's Guide EU Declaration of Conformity All relevant documentation is available for download from www.picotech.com/downloads

Compatible thermocouples

The USB TC-08 is compatible with all commonly used thermocouples, offering high accuracy without compromising acquisition speed. Thermocouple types and temperature ranges are shown in the table below.

Type	Overall range (°C)	0.1 °C resolution	0.025 °C resolution
B	20 to 1820	150 to 1820	600 to 1820
E	–270 to 910	–270 to 910	–260 to 910
J	–210 to 1200	–210 to 1200	–210 to 1200
K	–270 to 1370	–270 to 1370	–250 to 1370
N	–270 to 1300	–260 to 1300	–230 to 1300
R	–50 to 1760	–50 to 1760	20 to 1760
S	–50 to 1760	–50 to 1760	20 to 1760
T	–270 to 400	–270 to 400	–250 to 400

Also measures voltage and current!

The optional USB TC-08 single-channel terminal board plugs into one channel on the data logger and has a set of screw terminals, allowing you to connect sensors with voltage or current outputs to the data logger without any need for soldering. The four input ranges (±50 mV, ±500 mV, ±5 V and 4–20 mA) allow you to measure a wide range of signals.

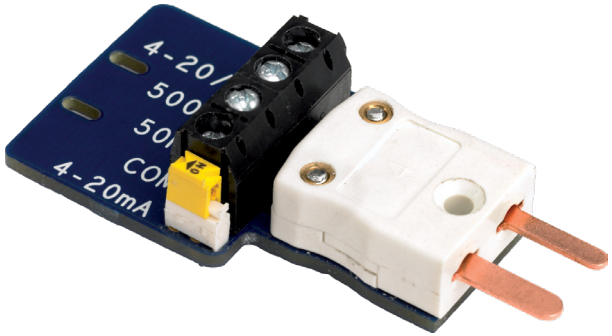

Ordering information

Pico offers both off-the-shelf and built-to-order thermocouples for use with the USB TC-08. If you require a custom build for your application, our Technical Support team is available to discuss your requirements. You can contact the team via email (support@picotech.com),

Type K and T thermocouples

Product name	Description
SE059 thermocouple type K	High-temperature, exposed tip, fiberglass insulated, 1 m
SE060 thermocouple type K	High-temperature, exposed tip, fiberglass insulated, 2 m
SE061 thermocouple type K	High-temperature, exposed tip, fiberglass insulated, 3 m
SE062 thermocouple type K	High-temperature, exposed tip, fiberglass insulated, 5 m
SE002 thermocouple type K	Probe, air, 4.5 mm tip
SE001 thermocouple type K	Exposed tip, fiberglass insulated, 1 m
SE030 thermocouple type K	Exposed tip, fiberglass insulated, 2 m
SE031 thermocouple type K	Exposed tip, fiberglass insulated, 5 m
SE000 thermocouple type K	Exposed tip, PTFE insulated, 1 m
SE027 thermocouple type K	Exposed tip, PTFE insulated, 2 m
SE028 thermocouple type K	Exposed tip, PTFE insulated, 3 m
SE029 thermocouple type K	Exposed tip, PTFE insulated, 10 m
SE003 thermocouple type K	Insertion, 3.3 mm tip
SE004 thermocouple type K	Ribbon surface, 8 mm tip
SE056 thermocouple type T	5 mm × 50 mm stainless steel waterproof tip, silicone insulated, 3 m
SE057 thermocouple type T	5 mm × 50 mm stainless steel waterproof tip, silicone insulated, 5 m
SE058 thermocouple type T	5 mm × 50 mm stainless steel waterproof tip, silicone insulated, 10 m
SE051 thermocouple type T	Exposed tip, fiberglass insulated, 1 m
SE052 thermocouple type T	Exposed tip, fiberglass insulated, 2 m
SE053 thermocouple type T	Exposed tip, fiberglass insulated, 3 m
SE054 thermocouple type T	Exposed tip, fiberglass insulated, 5 m
SE055 thermocouple type T	Exposed tip, fiberglass insulated, 10 m
SE046 thermocouple type T	Exposed tip, PTFE insulated, 1 m
SE047 thermocouple type T	Exposed tip, PTFE insulated, 2 m
SE048 thermocouple type T	Exposed tip, PTFE insulated, 3 m
SE049 thermocouple type T	Exposed tip, PTFE insulated, 5 m
SE050 thermocouple type T	Exposed tip, PTFE insulated, 10 m

Ordering information (continued)

Product name	Description
USB TC-08	Thermocouple data logger with Pico blue USB 2.0 cable, 1.8 m

Optional accessories

Product name	Description
USB TC-08 single-channel terminal board	Single-channel terminal board for use with USB TC-08 thermocouple data logger
USB 2.0 cable, 1.8 m*	Replacement Pico blue USB 2.0 cable, 1.8 m
USB 2.0 cable, 0.5 m*	Pico blue USB 2.0 cable, 0.5 m
USB 2.0 cable, 4.5 m*	Pico blue USB 2.0 cable, 4.5 m

* Pico blue USB cables are designed and built specifically for use with Pico Technology oscilloscopes and data loggers in order to minimize voltage drop and noise. Take care to use your USB TC-08 data logger with Pico blue USB cables only.

UK global headquarters:

Pico Technology
James House
Colmworth Business Park
St. Neots
Cambridgeshire
PE19 8YP
United Kingdom

☎ +44 (0) 1480 396 395
📠 +44 (0) 1480 396 296
✉ sales@picotech.com

North America regional office:

Pico Technology
320 N Glenwood Blvd
Tyler
Texas 75702
United States

☎ +1 800 591 2796
📠 +1 620 272 0981
✉ sales@picotech.com

Asia-Pacific regional office:

Pico Technology
Room 2252, 22/F, Centro
568 Hengfeng Road
Zhabei District
Shanghai 200070
PR China

☎ +86 21 2226-5152
✉ pico.china@picotech.com

THE QUEEN'S AWARDS FOR ENTERPRISE: INTERNATIONAL TRADE 2014

www.picotech.com

Pico Technology | @LifeAtPico | @picotechnologyltd | Pico Technology | @picotech

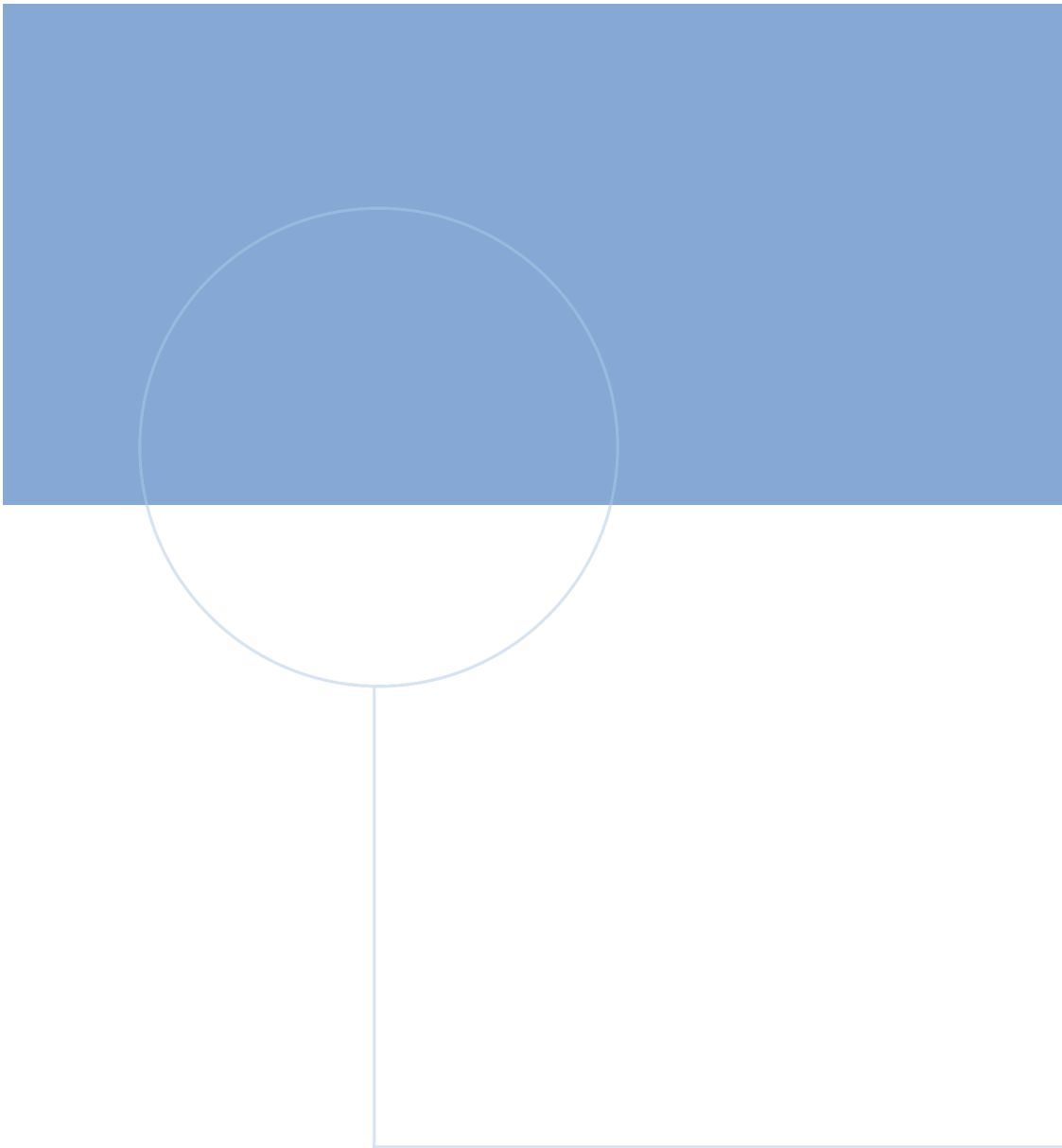

NTNU

Norwegian University of
Science and Technology